



UNITÉ DE RECHERCHE  
INRIA-SOPHIA ANTIPOLIS

Institut National  
de Recherche  
en Informatique  
et en Automatique

Domaine de Voluceau  
Rocquencourt  
B.P.105  
78153 Le Chesnay Cedex  
France  
Tél.: (1) 39 63 55 11

Rapports de Recherche

1 9 9 2



ème

anniversaire

N° 1584

*Programme 6*

*Calcul Scientifique, Modélisation et  
Logiciel numérique par Ordinateur*

**DESIGN OF AN ESSENTIALLY  
NON-OSCILLATORY  
RECONSTRUCTION PROCEDURE ON  
FINITE-ELEMENT TYPE MESHES**

**Rémi ABGRALL**

**Janvier 1992**



★ R R - 1 5 8 4 ★

Design of an Essentially Non-Oscillatory  
Reconstruction Procedure on Finite-Element Type  
Meshes

Définition d'un algorithme de reconstruction  
essentiellement non-oscillante sur des maillages non  
structurés

Rémi Abgrall  
INRIA, 2004, route des Lucioles, Sophia Antipolis,  
06560 Valbonne, France

### **Abstract**

In this report, we have designed an Essentially Non Oscillatory reconstruction for functions defined on finite-element type meshes. Two related problems are studied : the interpolation of possibly unsmooth multivariate functions on arbitrary meshes and the reconstruction of a function from its averages in the control volumes surrounding the nodes of the mesh. Concerning the first problem, we have studied the behaviour of the highest coefficients of two polynomial interpolations of a function that may admit discontinuities of locally regular curves : the Lagrange interpolation and an approximation such that the mean of the polynomial on any control volume is equal to that of the function to be approximated. This enables us to choose the best stencil for the approximation. The choice of the smallest possible number of stencils is addressed. Concerning the reconstruction problem, two methods have been studied : a first one based on an adaptation of the so-called reconstruction via deconvolution method to irregular meshes and a second one that lies on the approximation on the mean as defined above. The first method is conservative up to a quadrature formula and the second one is exactly conservative. The two methods have the expected order of accuracy, but the second one is much less expensive than the first one.

Some numerical examples are given which demonstrate the efficiency of the reconstruction

## Résumé

Dans ce rapport, nous définissons un algorithme de reconstruction essentiellement non oscillant pour des fonctions définies sur des maillages de type éléments finis. Deux problèmes sont étudiés : celui de l'interpolation sur un maillage arbitraire d'une fonction (ou l'une de ses dérivées) pouvant admettre des discontinuités et celui de la reconstruction de cette fonction à partir de la donnée de ses valeurs moyennes dans des cellules de contrôle autour des nœuds du maillage.

Deux type d'approximations polynomiales sont étudiées : l'interpolation par polynômes de Lagrange et une approximation où l'on impose les valeurs moyennes dans des cellules de contrôle.

Dans les deux cas, on a étudié le comportement des coefficients du polynôme d'approximation, en particulier dans le cas où la fonction qui est donnée admet des discontinuités situées sur des courbes régulières par morceaux.

Ces résultats, qui généralisent des résultats classiques, permettent d'obtenir un critère de détection des zones de régularité d'une fonction ; dont on a déduit la construction d'une interpolation essentiellement non oscillante.

Le problème de la reconstruction non oscillante à partir des valeurs moyennes est aussi abordé. Deux techniques sont proposées : la première qui utilise une méthode de déconvolution et la seconde qui utilise l'approximation polynomiale à partir des valeurs moyennes. Le premier type de reconstruction n'est conservatif qu'à une formule de quadrature près tandis que la seconde l'est formellement. Son coût est aussi bien moindre.

Le problème du choix d'un ensemble minimal de stencils permettant l'interpolation ou la reconstruction est aussi traité. On présente un critère heuristique, qui, pour tous les exemples que nous avons traités, semble suffisant.

# Contents

<b>1</b>	<b>Two approximations by polynomials in <math>\mathbb{R}^2</math></b>	<b>7</b>
1.1	The polynomials in $\mathbb{R}^2$ . . . . .	7
1.2	The approximation problem in $\mathbb{R}^2$ . . . . .	8
1.2.1	Determination of the polynomial expansion . . . . .	10
1.3	A recurrence formula . . . . .	11
1.4	Approximation of smooth and unsmooth function by polynomials . . . . .	13
1.4.1	Case of a "smooth" stencil . . . . .	14
1.4.2	Case of an "unsmooth" stencil . . . . .	17
<b>2</b>	<b>An E.N.O. Reconstruction Technique</b>	<b>23</b>
2.1	Non oscillatory interpolation . . . . .	24
2.2	Two conservative ENO reconstruction . . . . .	26
2.2.1	Deconvolution technique revisited . . . . .	26
2.2.2	A formally conservative reconstruction . . . . .	28
2.3	Some remarks for the practical calculation of the reconstruction . . . . .	28
<b>3</b>	<b>Numerical examples</b>	<b>30</b>

# List of Figures

2.1	Stencil and discontinuity curve . . . . .	36
2.2	Control volume around the node $i$ . . . . .	36
2.3	Some possible interpolation points. Circles : points of $T_{min}$ (second order interpolation), black circles : points that may be added to obtain a stencil for third order interpolation. . . . .	37
2.4	Construction of a stencil for fourth order approximation : the black circles represent the points to be added to a stencil for third order approximation (circles). The standard $P_3$ stencil is shown. . . . .	38
3.5	Typical mesh. 1600 nodes, 3042 triangles. . . . .	39
3.6	Exact function. Min=-1.331, Max=2.650, $\delta = 0.1$ . . . . .	40
3.7	$L^\infty$ error for $f(x, y) = \cos [2\pi(x^2 + y^2)]$ . Squares : E.N.O. interpolation only, Circles : E.N.O. + reconstruction. Dashed line : slope -3 . . . . .	41
3.8	$L^\infty$ error for $f(x, y) = \cos [2\pi(x^2 + y^2)]$ . Squares : Dashed line : slope -4, Dashed+squares : E.N.O. + reconstruction . . . . .	42
3.9	E.N.O. reconstruction "in the mean" with the 1600 nodes mesh. Min=-1.30, Max=2.6, $\delta = 0.1$ . . . . .	43
3.10	E.N.O. reconstruction "in the mean" with the 6400 nodes mesh. Min=-1.30, Max=2.6, $\delta = 0.1$ . . . . .	44
3.11	3th order E.N.O. reconstruction with the 6400 nodes mesh from the deconvolution technique. Min=-1.325, Max=2.650, $\delta = 0.8281 \cdot 10^{-2}$ . . . . .	45
3.12	Cross-section at $Y = 0$ of the E.N.O interpolation (a) and the E.N.O. reconstruction (b) for 1600 nodes the mesh. . . . .	46
3.13	Cross-section at $Y = 0.75$ of the E.N.O interpolation (a) and the E.N.O. reconstruction (b) for the 1600 nodes mesh. . . . .	47
3.14	Cross-section at $Y = -0.45$ of the E.N.O interpolation (a) and the E.N.O. reconstruction (b) for the 1600 nodes mesh. . . . .	48

# Notations

- $\mathbb{R}_n[X, Y]$  : finite dimensional vector space of two variable polynomials over  $\mathbb{R}$ ,
- $N(n) = \frac{(n+1)(n+2)}{2}$  : dimension of  $\mathbb{R}_n[X, Y]$ ,
- $S^{(n)}$  admissible stencil for solving the Lagrange problem in  $\mathbb{R}_n[X, Y]$ , see section 1.2,
- $||U||$  is the euclidian norm of  $U$ ,
- $D_{i,j}u = \frac{\partial^l u}{\partial^i x \partial^j y}$  where  $i + j = l$ ,
- $D^n u$  :  $n$ -th derivative of  $u$ .
- $\langle u \rangle_{C_i} = \frac{\int_{C_i} u(x) dx}{area(C_i)}$

# Introduction

During the past few years, a growing interest has emerged for building high order accurate schemes (i.e of order greater than 2) for compressible flows simulations. It is well known that even for smooth initial conditions, these flows may develop discontinuities that make linear schemes useless.

At the beginning of the 80's, the class of Total Variation Diminishing schemes appeared and they have been successfully and widely used with many types of meshes (see for example, [1] for a review and, among many others, [2] for simulations on finite element type meshes). Nevertheless, one of their main weaknesses is that the order of accuracy falls to first order in regions of discontinuity and at extrema, leading to excessive numerical dissipation.

Various methods have been proposed to overcome this difficulty (adaptation of the mesh for example) but one promising way may also be the class of the Essentially Non-Oscillatory schemes (E.N.O. for short) introduced by Harten, Osher and others [3,4,5,6,7].

The basic idea of E.N.O schemes is to use a Lagrange type interpolation with an adapted stencil : when a discontinuity is detected, the procedure looks for the region around this discontinuity where the function is the smoothest. Then a reconstruction technique may be applied which enables approximation of the function to any desired order of accuracy from its averages in control volumes surrounding the mesh points. The approximation is done so that it is conservative.

Some attempts have been made to extend these ideas to multidimensional flows (see for example [9]), but only for structured meshes.

In this report, we intend to study the problem of the reconstruction, up to any order of accuracy, of a given function given either by its value at the nodes of a triangulation or by its averages on control volumes defined around these nodes so that, in the second case, the reconstruction is conservative. This latter problem has already been studied, for smooth functions only, by Barth et al. [10].

The outline of this report is as follows. In the first part, we consider two ways of approximating functions by means of polynomials : the Lagrange interpolation and a approximation that conserves the mean on control volumes surrounding given points. In particular, we study the problem of the localization of region of smoothness from the coefficients of the polynomial. We recall the results concerning the approximation of smooth functions by Lagrange interpolation and we show that the same results are also true for the second approximation we consider in this paper. In the case of unsmooth functions (or more precisely the function which regions of possible unsmoothness lies on locally  $C^1$  curves), we give the asymptotic



behaviour of the coefficients of highest degree in the approximation. These latter results seem to be new.

Then we propose an algorithm for ENO interpolation. We try to give some indication for selecting the smallest of possible stencils for any order of accuracy. We also propose two algorithms for reconstructing a function from its mean values in control volume. The first one follows from an adaptation of the so-called reconstruction via deconvolution procedure that was originally built for regular meshes. We indicate why, in general, the conservation property is formally lost to ensure a high order of approximation when using deconvolution technique ; conservation up to a high order quadrature formula is guaranty. Then a secnd algorithm, directly inspired from Bath et al. [10] and Harten et al [8] is proposed and analysed. This latter one ensure formal conservation and, form a computational point of view, is much more economical than the first one.

Some numerical tests are proposed indicate the performance of the various methods.

# Chapter 1

## Two approximations by polynomials in $\mathbb{R}^2$

### 1.1 The polynomials in $\mathbb{R}^2$

We will denote by  $\mathbb{R}[X, Y]$  the vector space of the polynomials of two variables ( $X$  and  $Y$ ) with coefficients in  $\mathbb{R}$ . An element of  $\mathbb{R}[X, Y]$  may be described by its (finite) expansion in terms of powers of  $X$  and  $Y$  :

$$P(X, Y) = \sum_{l=1}^n \sum_{i+j=l, i,j \geq 0} a_{i,j} X^i Y^j \quad (1.1)$$

The highest integer such that at least one of the coefficients of the monomials  $X^i Y^j$  is non zero is called the *total degree* of  $P$ .

If  $(x_0, y_0)$  is a point of  $\mathbb{R}^2$ , another expansion of  $P$  may be written in terms of the monomials  $(X - x_0)^i (Y - y_0)^j$  with the help of the Taylor formula. The total degree of  $P$  does not depend on the point  $(x_0, y_0)$ .

In the sequel, we will denote by  $\mathbb{R}_n[X, Y]$  the (finite) vector space of the polynomials of  $\mathbb{R}[X, Y]$  with total degree less or equal to  $n$ . This vector space has dimension  $N(n) = \frac{(n+1)(n+2)}{2}$ , a basis of which is the set of monomials  $(X - x_0)^i (Y - y_0)^j$  of total degree  $i + j$  less or equal to  $n$ .

Let us now describe another interesting basis of  $\mathbb{R}_n[X, Y]$ . Consider  $(A, B, C)$  a triangle of  $\mathbb{R}^2$  and let us denote by  $\Lambda_A, \Lambda_B, \Lambda_C$  the barycentric coordinates of the three points  $(A, B, C)$  defined, for any point  $M$ , by :

$$\begin{aligned} M &= \Lambda_A A + \Lambda_B B + \Lambda_C C \\ \Lambda_A + \Lambda_B + \Lambda_C &= 1 \end{aligned} \quad (1.2)$$

It is easy to see that, for any pair of points, say  $A$  and  $B$ , the set  $\{\Lambda_A^i \Lambda_B^j\}_{i+j \leq n}$  is also a basis of  $\mathbb{R}_n[X, Y]$ .

## 1.2 The approximation problem in $\mathbb{R}^2$

Throughout this paper, we will consider the following approximation problem : let us consider the following problem ( $\mathcal{I}$ ) defined for regular enough real valued functions on  $\mathbb{R}^2$  :

*Given  $N$  and  $n$ , two integers, a family  $(L_i)_{1 \leq i \leq n}$  of  $N$  linear forms defined on  $C^p(\mathbb{R}^2)$  ( $p > n$ ), find an element  $P$  of  $\mathbb{R}_n[X, Y]$  such that for any point  $i$ , one has  $L_i(P) = L_i(u)$  for  $1 \leq i \leq N$ .*

In the sequel, two kind of linear forms are considered :

- if  $\mathcal{S}^{(n)} = (A_i)_{1 \leq i \leq N}$  is a family of  $N$  points in  $\mathbb{R}^2$ , the first approximation (Lagrange interpolation) is associated with :

$$L_i(u) = u(A_i), \quad 1 \leq i \leq N,$$

- if  $(A_i)_{1 \leq i \leq N}$  is a family of  $N$  points in  $\mathbb{R}^2$  and if  $\{C_i, 1 \leq i \leq N\}$  is a family of control volume around the nodes  $A_i$ , the second approximation we consider is associated with :

$$L_i(u) = \langle u \rangle_{C_i}.$$

In this second case, we set  $\mathcal{S}^{(n)} = (A_i, C_i)_{1 \leq i \leq N}$ . This set will be also called a “stencil” (though this is not very appropriate in this case) in order to simplify the text.

In the sequel, we will often make no distinction between a point element  $A_i$  of  $\mathcal{S}^{(n)}$  and its coordinates in a suitable frame,  $(x_i, y_i)$ . We always assume that the control volume satisfies the following properties :

1.  $C_i \cap C_j$  is of empty interior when  $i \neq j$  (generally speaking, a collection of segments or an empty set),
2.  $C_i$  is connex,
3. we assume that there is a continuous dependency of  $C_i$  in term of the points of the stencil. This guaranties in particular that the area of  $C_i$  and the mean values of  $X^i Y^j$  on  $C_i$  depend continuously of the points of the stencil.

Some examples of control volume are shown in section 2.

For this problem to have a solution, two conditions must be fulfilled :

1. one must have  $N = \frac{(n+1)(n+2)}{2}$

2. the following generalized Van der Monde determinant must be non zero :

$$\Delta_{\mathcal{S}^{(n)}} = \det [L_i(X^i Y^j)] \Big|_{\substack{i+j \leq n \\ 1 \leq l \leq N}} = \begin{vmatrix} L_1(1) & L_1(X) & L_1(Y) & \cdots & L_1(X^n) & L_1(X^{n-1}Y) & \cdots & L_1(Y^n) \\ \vdots & \vdots & \vdots & \vdots & \vdots & \vdots & \vdots & \vdots \\ L_N(1) & L_N(X) & L_N(Y) & \cdots & L_N(X^n) & L_N(X^{n-1}Y) & \cdots & L_N(Y^n) \end{vmatrix} \quad (1.3)$$

We will say that the set  $\mathcal{S}^{(n)}$  is *admissible* if  $\Delta_{\mathcal{S}^{(n)}} \neq 0$ . If a set  $\mathcal{S}^{(n)}$  is admissible, for any function  $u$  there exist  $\frac{(n+1)(n+2)}{2}$  coefficients,  $(a_{i,j})$ , such that the solution of the problem (I) is :

$$P = \sum_{l=1}^n \sum_{i+j=l, i,j \geq 0} a_{i,j} X^i Y^j. \quad (1.4)$$

In the sequel, the polynomial  $P$  will often be denoted as  $\Pi_L(u)$  in the case of the Lagrange interpolation (i.e  $L_i(u) = u(A_i)$ ) and  $\Pi_M(u)$  in the case of the approximation in the mean (i.e  $L_i(u) = \langle u \rangle_{C_i}$ ).

The problem of characterizing the admissible sets for the Lagrange interpolation has been widely studied, see [11] for example and the references therein. We do not know any criteria for selecting admissible stencils for the approximation in the mean.

**Remarks :**

1. The condition (1.3) has been given for the basis  $X^i Y^j$  of  $\mathbb{R}_n[X, Y]$ . A similar and equivalent condition could have been given for the two other bases we have mentioned. The formula (1.4), provided that the monomials  $X^i Y^j$  are replaced by the elements of the new basis, is also true.
2. If  $\text{card } \mathcal{S}^{(1)} = 3$  and if the Lagrange problem is considered, this condition is nothing more than the one which says that the three points must not be aligned.
3. If we were in  $\mathbb{R}$ , this determinant, for the Lagrange problem, would be the classical van der Monde determinant.
4. In the case of the Lagrange problem, the set of  $\frac{(n+1)(n+2)}{2}$ -uplets where the condition (1.3) is not fulfilled is an algebraic curve of  $\mathbb{R}^{N^{(n)}}$  and consequently a closed subset of measure zero in  $\mathbb{R}^{N^{(n)}}$ . In the second case, this is also true, at least for the kind of control volume we consider wick boundary are made of segments, the equation of which depend linearly of the coordinates of the nodes of  $\mathcal{S}^{(n)}$ .

In the next section, we address the question of the practical calculation of the coefficients  $a_{i,j}$ .

### 1.2.1 Determination of the polynomial expansion

In this section, we use the monomials  $X^i Y^j$  for expanding polynomials, but any other basis would be suitable and the results are immediately transposable.

The coefficients of the Lagrange expansion are the solution of the linear  $N(n) \times N(n)$  system :

$$L_l(u) = \sum_{i=1}^n \sum_{i+j=l, i,j \geq 0} a_i, L_l(X^i Y^j) \quad \text{for all } 1 \leq l \leq N \quad (1.5)$$

This Lagrange type interpolation problem have been considered by several authors, among which Muhlbach [12,13].

Since condition (1.3) is true, the Cramer formula applied to (1.5) gives the answer, but this solution is not computationally very efficient. Several authors have tried to generalize the Newton formula that make the Lagrange interpolation in  $\mathbb{R}$  efficient from a numerical point of view, and a very general answer has been given by Muhlbach [12,13].

In these papers, he addresses the problem of the "interpolation" by a set of functions  $(f_i)_{i \in I}$  such that the property (I) is true. He calls the set  $(f_i)$  a *Cebysev-system* if given any function  $f$ , for any pair of subsets of  $I$ ,  $L$  and  $M$ , having the same (finite) number of elements, there exist real numbers  $\alpha_i$  such that :

$$u_i = \sum_{j \in M} \alpha_j L_j(f_j), \quad \text{for all } i \in L. \quad (1.6)$$

For the sake of clarity, we may assume that  $L = M = \{1, \dots, N\}$ . He uses the notation :

$$\left[ \begin{array}{c} f_1 \cdots f_k \\ L_1 \cdots L_k \end{array} \middle| f \right]$$

for denoting the coefficients of  $f_k$  in the development (1.6). Then, in [13], he shows that if one has a Chebysev system (theorem 4.1 pp. 106) :

$$\left[ \begin{array}{c} f_1 \cdots f_n \\ L_1 \cdots L_n \end{array} \middle| f \right] = \frac{\left[ \begin{array}{c} f_1 \cdots f_{n-1} \\ L_2 \cdots L_n \end{array} \middle| f \right] - \left[ \begin{array}{c} f_1 \cdots f_{n-1} \\ L_1 \cdots L_{n-1} \end{array} \middle| f \right]}{\left[ \begin{array}{c} f_1 \cdots f_{n-1} \\ L_2 \cdots L_n \end{array} \middle| f \right] - \left[ \begin{array}{c} f_1 \cdots f_{n-1} \\ L_1 \cdots L_{n-1} \end{array} \middle| f \right]}. \quad (1.7)$$

This expression is a direct generalization of the classical Newton formula. Let us make several comments on this formula when applied to our problem :

1. If one adopts the lexicographic ordering  $1, X, Y, X^2, XY, Y^2, \dots, X^n, X^{n-1}Y, \dots, XY^{n-1}, Y^n$ , the previous formula (1.7) must be applied  $n+1$  times to go from a total degree  $n$  to a total degree  $n+1$ . One must also store quite a lot of terms like

$$\left[ \begin{array}{c} f_1 \cdots f_k \\ L_1 \cdots L_k \end{array} \middle| f \right]$$

to build the divided difference table. For example, to go from degree one to degree two, one must evaluate and store  $C_6^3$  approximations of gradients by mean of approximations on triangles, combine them to obtain approximation on sets of four points ( $C_6^4$  sets), five points ( $C_6^5$  sets) and six points (one set). Moreover, to go from approximation on  $k$  points to  $k + 1$  points,  $(k + 1) \times (k + 1)$ -determinants must be evaluated.

2. From a numerical point of view, the basis  $X^i Y^j$  or  $(X - a)^i (Y - b)^j$  are not well suited to calculations. This can easily be seen since for any pair  $(a, b)$ ,

$$\left[ L(X^i Y^j) \right]_{\substack{i+j \leq n \\ 1 \leq l \leq N}} = \left[ L_l[(x - a)^i (y - b)^j] \right]_{\substack{i+j \leq n \\ 1 \leq l \leq N}} .$$

If  $(a, b)$  is any point of  $\mathcal{S}^{(n)}$  and if  $h = \max_{(x_l, y_l) \in \mathcal{S}^{(n)}} (|x_l - a|, |y_l - b|)$ , because for both kind of linear forms we consider here, we have  $|L_l[(X - a)^i (Y - b)^j]| \leq h^{i+j}$ , Hadamard's inequality shows that :

$$|\Delta_{\mathcal{S}^{(n)}}| \leq h^{\kappa(n)},$$

where  $\kappa(n) = 1 + \sum_{l=1, n}^p \frac{(p+1)(p+2)}{2} = O(n^4)$  so that one reaches very quickly machine zero though the linear system may be well conditioned.

An alternative to this last point is to use local coordinates such as the barycentric ones. In the E.N.O. method we will develop in a further section, for each point, the natural barycentric coordinates are not known *a priori* so that the work has to be repeated at each interpolation call. If this is included in an iterative algorithm, the cost (and the storage) seems to be much too important at least for the cases we have considered in this report. For all these reasons, we have preferred to use classical inversion techniques for linear systems.

### 1.3 A recurrence formula

In this section, we wish to show another recurrence formula that enables us to obtain the coefficients of the expansion of total degree  $n$  from those of the expansion of total degree less than  $n$  in only one step. This recurrence formula may probably be viewed as another version of that given in [13], theorem 3.1, page 400 and will be useful in section 1.4.

Let us begin with some notations. Let  $P_1, \dots, P_{N(n)}$  be a basis of  $\mathbb{R}_n[X, Y]$  such that  $P_1, \dots, P_{N(p)}$ ,  $p < n$ , is a basis of  $\mathbb{R}_p[X, Y]$ . The three basis we have considered in section 1.2 are of that kind. Let  $\mathcal{S}^{(n)}$  be an admissible stencil. We set :

$$R_l = \left( L_l(P_1) \cdots L_l(P_{N(n)}) \right)^T$$

so that the solution of the Lagrange-type problem  $(\mathcal{I})$  (where the  $u_i$ 's are given),

$$u_i = \sum_{1 \leq j \leq N(n)} \alpha_j L_i(P_j) \quad \text{for all } i,$$

may be seen as the solution of the linear system

$$\mathcal{M} \left( \alpha_1 \cdots \alpha_{N(n)} \right)^T = U = \left( u_1 \cdots u_{N(n)} \right)^T, \quad (1.8)$$

where the  $l$ -th row of  $\mathcal{M}$  is  $R_l$ . The solutions of system (1.8) are :

$$\alpha_l^{(n)} = \frac{\det(R_1 \cdots \widehat{R}_l \cdots R_{N(n)})}{\det(R_1 \cdots R_l \cdots R_{N(n)})}, \quad (1.9)$$

where  $\widehat{R}_l = U$  denotes the  $l$ -th column.

**Lemma 1.3.1** *Let  $(A_i)_{1 \leq i \leq N(n)}$  be an admissible set in which any of its  $N(p), p \leq n$ , subsets is admissible. Then, for a given  $p < n$ , let  $I = \{i_1, \dots, i_{N(p)}\}$  and  $J$  be ordered sets such that  $I \cup J = \{1, \dots, N(n)\}$ . If  $A = (a_{ij})$  is a  $N(n) \times N(n)$  matrix, we set*

$$\det(A)_I = \det(a_{ij}) \Big|_{\substack{1 \leq i \leq N(p) \\ j \in I}},$$

and  $\det(A)_{J,I} = \det(a_{ij}) \Big|_{\substack{N(p)+1 \leq i \leq N(n) \\ j \in J}}.$

Let us also denote by  $\alpha_{I'}^{(p)}$  the coefficient of  $P^{(p)}$  of the Lagrange problem of degree  $p$  for nodes in  $I$  (for degree  $n$ , we omit the subscript  $I$ ).

Then for any  $l' \leq N(p)$ , we have

$$\alpha_l^{(n)} = \sum_{I, \text{card}(I)=N(p)} \lambda_I^{l'} \alpha_{I'}^{(p)}$$

$$\lambda_I^{l'} = (-1)^{\sigma(I)} \frac{\det(R_1 \cdots R_{l'} \cdots R_{N(p)})_I \det(R_{N(p)+1} \cdots R_{l'} \cdots R_{N(n)})_J}{\det(R_1 \cdots R_{N(n)})}, \quad (1.10)$$

where  $\sigma(I) = 1 + p(p+1)/2 + \sum_{i \in I} i$ . In (1.10),  $R_{l'}$  appears a first time at the  $l'$ -th row of  $\det(R_1 \cdots R_{l'} \cdots R_{N(p)})_I$  and a second time at the  $l - N(p)$ -th row of  $\det(R_{N(p)+1} \cdots R_{l'} \cdots R_{N(n)})_J$ .

**Proof :** By switching columns  $l$  and  $l'$  in (1.9), one gets :

$$\alpha_l^{(n)} = - \frac{\det(R_1 \cdots \widehat{R}_l \cdots R_{l'} \cdots R_{N(n)})}{\det(R_1 \cdots R_l \cdots R_{N(n)})}.$$

Then, a direct application of the generalized Lagrange formula (see [14], pp 19-22) to the previous expression gives

$$\det(R_1, \dots, \widehat{R}_l \cdots R_{l'} \cdots R_{N(n)}) =$$

$$\sum_{I, \text{card}(I)=N(p)} (-1)^{\sigma(I)} \det(R_1 \cdots \widehat{R}_l \cdots R_{N(p)})_I \det(R_{N(p)+1} \cdots R_{l'} \cdots R_{N(n)})_J$$

Since any  $N(p)$  subset is admissible, one has

$$\alpha_{l'}^{(p)} = \frac{\det(R_1 \cdots \widehat{R_l} \cdots R_{N(p)})_I}{\det(R_1 \cdots R_{l'} \cdots R_{N(n)})_I},$$

and the results follows immediately. •

**Lemma 1.3.2** *With the assumptions of lemma 1.3.1, then, for  $p < n$ , if  $N(p) \leq l \leq N(n)$  and  $l' < N(p)$ ,*

$$\sum_{I, \text{card}(I)=N(p)} \lambda_I^{l'} = 0.$$

**Proof :** Apply the Lagrange formula to

$$\det(R_1 \cdots R_{l'} \cdots R_{N(p)} R_{N(p)+1} \cdots R_l R_{N(n)}) = 0,$$

and interpret the coefficients in terms of  $\alpha$ 's, all equal to 1, and  $\lambda$ 's. The lemma 1.3.1 gives the result •

## 1.4 Approximation of smooth and unsmooth function by polynomials

The problem of interest in this section is the following : Let  $u$  be a real function defined on an open subset  $\Omega$  of  $\mathbb{R}^2$ . We assume that  $u$  is  $n$  times continuously differentiable on  $\Omega$  except perhaps on a subset of  $\Omega$  consisting of a finite collection of locally  $C^1$  curves. Let now  $\mathcal{T}$  be a mesh. For each point of  $\mathcal{T}$ , we consider one of the two Lagrange-type interpolation of  $u$  considered above. Is it possible to localize the regions of smoothness of  $u$  from the coefficients of the polynomial approximation of  $u$  ? The answer is yes if additional assumptions are made on the mesh. These assumptions guarantee that one can solve the problem (I) for any order from 1 to  $n$ , and may be seen as a very natural generalization of classical conditions used in the finite elements theory [15].

For functions defined on  $\mathbb{R}$ , one knows that the divided differences of  $u$  satisfy :

- If  $u$  is smooth on an interval  $I$  containing  $x_1, \dots, x_n$ , then there exists  $\xi \in I$  such that

$$[x_1, x_2, \dots, x_n | u] = \frac{f^{(n)}(\xi)}{n!},$$

- if  $u^{(k)}$  has a jump  $[u^{(k)}]$  on  $I$ , one has

$$[x_1, x_2, \dots, x_n | u] = O([u^{(k)}](x_n - x_1)^{k-n}).$$



In this section, we intend to generalize these relations, and in particular, the second one since this problem seems (surprisingly) not to have been studied yet. The proof appears to be rather technical. It is divided into two parts. In the first part, we study the case of a stencil  $S^{(n)}$  of  $N(n)$  points where  $u$  admits two values, 0 and 1. We give the asymptotic behaviour of the highest coefficient of the polynomial of degree  $n$  that approximates  $u$  when it is *exactly* of total degree  $n$ . Then, we define a condition on the stencils that appears to be a generalization of the one that says that triangles must not have too small angles to ensure a uniform error bound for classical finite elements [15]. Then, using Lemmas 1.3.1 and 1.3.2, we obtain our result. Let us begin with the case of a stencil in which convex hull  $u$  is smooth. We first recall the results of Ciarlet and Raviart for Lagrange interpolation and we show that their proof is also true for the second kind of approximation, so that a high order of approximation is ensured.

#### 1.4.1 Case of a "smooth" stencil

This problem, for Lagrange and Hermite interpolation, has been studied by for example Ciarlet and Raviart in [16]. As we show it in the paragraph 1.4.1, their error study of the Lagrange interpolation can easily be extended to the second problem we consider in this paper. In the following theorem,  $K$  denotes the convex hull of the points of the stencil  $S^{(n)}$  in the case of the lagrange interpolation and the convex hull of the reunion of the control volumes  $C_i$  for the approximation in the mean.

**Theorem 1.4.1** *Let  $S^{(n)}$  be an admissible (for degree  $n$ ) stencil of  $\mathbb{R}^2$ , and let  $h$  and  $\rho$  be respectively the diameter of  $K$  and the supremum of the diameters of the spheres contained in  $K$ . Let  $u$  be a function that admits everywhere in  $K$  a  $n + 1$ th derivative  $D^{n+1}u$  with*

$$M_{n+1} = \sup\{\|D^{n+1}u(x)\|; x \in K\} < +\infty.$$

*If  $\Pi$  denotes either  $\Pi_L$  or  $\Pi_M$ , the projectors on the space of polynomials of degree less than  $n$ , we have for any integer  $m$  with  $0 \leq m \leq n$ ,*

$$\sup\{\|D^m u(x) - D^m \Pi(u)(x)\|; x \in K\} \leq CM_{n+1} \frac{h^{n+1}}{\rho^m},$$

*for some constants*

$$C = C(n, m, S^{(n)}).$$

*Moreover, if  $S^{(n)'}$  is obtained from  $S^{(n)}$  by an affine transformation, then  $C(n, m, S^{(n)}) = C(n, m, S^{(n)'})$ .*

From this inequality, one sees that the "flatter"  $K$  is, the poorer the estimation is. A direct application of this theorem gives a generalization of our first statement.

### Proof of the error estimate for approximations in the mean

The proof of this results is directly inspired form Ciarlet & Raviart without almost any change. In all what follows,  $K$  denotes the convex hull of  $\bigcup_{1 \leq i \leq N(n)} C_i$ .

**Lemma 1.4.2** *Let  $n \geq 1$  be an integer number, let us assume that  $\mathcal{S}^{(n)} = (a_i, C_i)_{1 \leq i \leq N(n)}$  is admissible and let  $u \in C^p$  with  $p > n$ . Then, for any  $x \in K$  and for any integer  $m$ ,  $0 \leq m \leq n$ , one have :*

$$D^m \Pi(u) = D^m u + \frac{1}{m!} \sum_{1 \leq i \leq N(n)} \left[ D^{m+1} u(\nu_i(x)) (\alpha_i - x)^{k+1} \right] D^m p_i \quad (1.11)$$

where the  $p_i$ 's are the polynomials defined by

$$\langle p_i \rangle_{C_j} = \delta_{ij}^j,$$

the  $\alpha_i$ 's are some point of  $C_i$  and the  $\nu_i$ 's are

$$\nu_i(x) = \theta_i x + (1 - \theta_i) \alpha_i$$

for  $0 < \theta_i < 1$

**Proof :** The proof follows the one given by Ciarlet and Raviart in [16].

From the definition of the  $p_i$ 's, we have :

$$\Pi_M(u) = \sum_{i=1, N(n)} \langle u \rangle_{C_i} p_i$$

Since  $C_i$  is connex and  $u$  continuous on  $C_i$ , there exist some  $\alpha_i$  such that  $\langle u \rangle_{C_i} = u(\alpha_i)$  and consequently :

$$\Pi_M(u) = \sum_{i=1}^{N(n)} u(\alpha_i) p_i, \quad D^m \Pi_M(u) = \sum_{i=1}^{N(n)} u(\alpha_i) D^m p_i$$

Let  $x \in K$ . One apply the Taylor formula to order  $n$  :

$$u(\alpha_i) = u(x) + Du(x) \cdot (\alpha_i - x) + \cdots + \frac{1}{n!} D^n u(x) \cdot (\alpha_i - x)^n + \frac{1}{(n+1)!} D^{n+1} u(\nu_i(x)) \cdot (\alpha_i - x)^{n+1}$$

where  $\nu_i$  satisfies the conditions of lemma 1.4.2. From this, one obtain :

$$D^m \Pi_M(u) = \sum_{l=0}^n \frac{1}{l!} \sum_{i=1}^{N(n)} \left\{ D^l u(x) \cdot (\alpha_i - x)^l \right\} D^m p_i + \frac{1}{(n+1)!} \sum_{i=1}^{N(n)} \left\{ D^{n+1} u(\nu_i(x)) \cdot (\alpha_i - x)^{n+1} \right\} D^m p_i \quad (1.12)$$

As in [16], let us show now that :

$$\frac{1}{l!} \sum_{i=1}^{N(n)} \{ D^l u(x) \cdot (\alpha_i - x)^l \} D^m p_i = \begin{cases} 0 & \text{for } 0 \leq l \leq m-1 \\ D^m u(x) & \text{for } l = m \\ 0 & \text{for } m+1 \leq l \leq n \end{cases} \quad (1.13)$$

One first show that

$$\sum_{i=1}^{N(n)} \{ D^l u(x) \cdot (\alpha_i - x)^l \} D^m p_i = 0 \quad \text{for } l \in \{0, 1, \dots, m-1\}.$$

For  $m = 0$ , one notice that  $1 = \sum_{i=1}^{N(n)} p_i$  (because  $\Pi_M$  let the polynomials of total degree less than  $n > 0$  invariant), so that for any constant  $A_0$ ,

$$0 = \sum_{i=1}^{N(n)} A_0 D^m p_i,$$

and, in particular, for the constant function  $A_0 = u(x)$ . This shows (1.13) for  $l = 0$ .

The proof of (1.13) for  $l \leq m-1$  follows by induction : assume (1.13) for  $l = 0, 1, \dots, l_0$  with  $l_0 \leq m-2$ . If  $A_{l_0}$  is a constant  $l_0$ -multilinear symetric form on  $\mathbb{R}^2$ , one can associate to it a polynomial  $P$  such that  $D^{l_0} P = A_{l_0}$  ( $P = \frac{1}{l_0!} A_{l_0} \cdot x^{l_0}$ ). From (1.12), and from the induction assumption, one has :

$$0 = \sum_{i=1}^{N(n)} \{ A_{l_0} \cdot (\alpha_i - x)^{l_0} \} D^m p_i, \quad \text{for all } x \in \mathbb{R}^2$$

If one sets  $A_{l_0} = D^{l_0} u(x)$ , one gets (1.13) for  $l = l_0$  and the result is true for all  $l$ ,  $0 \leq l \leq m-1$ .

If  $l = m$ , if  $A_m$  is a constant  $m$ -multilinear symetric form on  $\mathbb{R}^2$ , since that  $\Pi_M$  let invariant the polynomials of degree less than  $n$ , the formula (1.12) combined with what we have just shown indicate that :

$$A_m = \sum_{i=1}^{N(n)} \{ A_m \cdot (\alpha_i - x)^m \} D^m p_i, \quad \text{for all } x \in \mathbb{R}^2$$

In particular for  $A_m = D^m u(x)$  and then (1.13) is true for  $l = m$ .

The proof for  $m+1 \leq n$  is similar and follows by induction. •

From that proof, one can see that the key point is the invariance of polynomials by  $\Pi_M$ , the fact that  $\sum_{i=1}^{N(n)} p_i = 1$  and the existence of the  $\alpha_i$ 's. Only that latter point is particular to the projection  $\Pi_M$  we have chosen here.

The rest of the proof of theorem for  $\Pi = \Pi_M$  is exactly as in [16], so that we only indicate the lemmas that are needed.

**Lemma 1.4.3** Let  $\widehat{S}^{(n)} = \{\widehat{a}_i, \widehat{C}_i\}$  be an admissible stencil. Let  $S^{(n)} = \{a_i, C_i\}$  be an equivalent stencil, i.e there exist a matrix  $B$  and a point  $x_0$  such that :

$$a_i = B\widehat{a}_i + x_0$$

$$C_i = B\widehat{C}_i + x_0$$

Then  $S^{(n)}$  is admissible.

**Lemma 1.4.4** If  $h$  is the diameter of  $K$  and  $\rho$  is the diameter of the circles contained in  $K$ , then, if  $\widehat{S}^{(n)}$  and  $S^{(n)}$  are two equivalent stencils,

$$\|B\| \leq \frac{h}{\rho}$$

$$\|B^{-1}\| \leq \frac{\widehat{h}}{\rho}$$

The combination of lemmas 1.4.3 and 1.4.4 combined with lemma 1.4.2 gives the theorem 1.4.1.

## 1.4.2 Case of an "unsmooth" stencil

### Study of a simplified problem

Let us consider  $S^{(n)}$  an admissible stencil of cardinality  $\frac{(n+1)(n+2)}{2}$  and  $S_0, S_1$  two non-empty subsets of  $S^{(n)}$  having empty intersection, the union of which is  $S^{(n)}$ . Let us consider a polynomial  $P$  of total degree  $n$  such that for all points of  $S_0$ ,  $P$  has value 0 and for those of  $S_1$ ,  $P$  has value 1. We define, for  $\epsilon > 0$ , the set  $\mathcal{P}_n^\epsilon$  of possible stencils for which the total degree of  $P$  is exactly  $n$  :

**Property 1.4.5** The stencil  $S^{(n)}$  belongs to  $\mathcal{P}_n^\epsilon$  if and only if, for any vector  $U$  which components are either 0 or 1 such that both values are represented,

$$\sum_{l=N(n-1)+1}^{N(n)} \left| \det \left( \frac{R_0}{\|R_0\|} \cdots \frac{R_{N(n-1)}}{\|R_{N(n-1)}\|} \cdots \widehat{R}_l \cdots \frac{R_{N(n)}}{\|R_{N(n)}\|} \right) \right| \geq \epsilon \quad (1.14)$$

where  $\widehat{R}_l = U$

In the definition of property 1.4.5, we have adopted the lexicographic ordering

**Remarks :**

- There are only  $2^{N(n)} - 2$  such vectors  $U$ , so that the number of conditions (1.14) remain finite.

- The condition (1.14) is homogeneous of degree 0.
- For first and second order approximation, we have the following result :

**Lemma 1.4.6** *If any subset of cardinality  $\frac{(k+1)(k+2)}{2}$ ,  $k \leq n$ , of is admissible, then the polynomial approximations are of maximal degree for  $n = 1, 2$*

**Proof :**

- Degree one. The stencil is made of three points  $A, B, C$  that make a triangle.  $P$  is either of type  $\Lambda_A$  or  $1 - \Lambda_A$  and is of degree exactly one.
- Degree 2. Let us assume that  $P$  is at most of degree 1. Set  $N = \text{card}(S_0)$  and  $M = S_1$ . We have  $N + M = N(2) = 6$ . One may assume that  $N \leq M$  by changing  $P$  into  $1 - P$ . So,  $2N \leq 6$ . Then, one can see that there is always, for degree 2, at least 3 points that have the same value. Since these three points are admissible for degree one and since by assumption,  $P$  is either a constant or of degree 1, we see that it *must* be a constant which is absurd since it takes two different values. •

The same argument applied to degrees  $n=3,4,5$  shows that  $P$  must be of degree exactly  $n - 1$  because we always have

$$\frac{(n+1)(n+2)}{4} \geq \frac{n(n+1)}{2},$$

but fails for degrees greater or equal to 6 (because the previous inequality does not hold if  $n > 5$ ).

With this in hand, we get the following result, if  $R_{i,j}$  is the following vector :

$$R_{i,j} = \left( L_1[(X - x_0)^i(Y - y_0)^j] \cdots L_N[(X - x_0)^i(Y - y_0)^j] \right)^T.$$

**Lemma 1.4.7** *Let  $(x_0, y_0)$  be any point of the convex hull  $K$  of  $S^{(n)}$ . Assume that the stencil satisfies property 1.4.5 for some  $\epsilon > 0$ . Let  $P$  be a polynomial that is 1 on  $S_1$  and 0 on  $S_0$ . If  $h = \max\{(|x_l - x_0|, |y_l - y_0|), (x_l, y_l) \in S^{(n)}\}$ , then there exist two constants  $C_1(n, \epsilon) > 0$  and  $C_2(n) > 0$  such that the coefficients of the Taylor expansion of  $P$  around  $(x_0, y_0)$  :*

$$P = \sum_{i+j \leq n} a_{i,j} (X - x_0)^i (Y - y_0)^j,$$

satisfy

$$C_2(n)h^{-n} \geq \sum_{i+j=n} |a_{i,j}| \geq C_1(n, \epsilon)h^{-n}. \quad (1.15)$$

**Proof :** We adopt the lexicographic ordering of monomials. The set of admissible stencils satisfying property (1.4.5) and  $|h| \leq C$  is a compact subset  $\mathcal{C}$  of  $\mathbb{R}^{N(n)}$  because the determinant is continuous and the values of the mean of  $X^i Y^j$  depend continuously of the point of the stencil. Let us consider the real functions defined on  $\mathcal{C}$  by :

$$\phi_{i,j}(A_1, \dots, A_N) = \sum_{i=1,n} |\det(R_{00} \dots U_{i,j} \dots R_{0n})|,$$

and

$$\psi_{ij}(A_1 \dots A_N) = \left| \frac{\det(R_{00} \dots V_{ij} \dots R_{0n})}{\det(R_1 \dots R_N)} \right|,$$

in which the vector  $U_{ij}$  stands at the " $ij$ "-th column and has the value

$$U_{ij} = (0, \dots, 1, \dots 0)^T$$

and also  $V_{i,j}$  be  $\sum_{i+j \leq n} P(A_{ij}) U_{ij}$  where the "1" is at the  $L$ -th position (we refer to the lexicographic order). Let us note that  $P(A_{ij})$  is zero or one, and its value depends only on  $ij$  and not  $\mathcal{S}^{(n)}$ .

It is clear that  $\psi_{ij}$  is the absolute value of the coefficient of  $(X - x_0)^i (Y - y_0)^j$  in the Taylor expansion of  $P$ . It is also clear that

$$h^{-(i+j)} |\det[R_{0,0} \dots R_{i,j} \dots R_{0,n}]| \leq \phi_{i,j},$$

by the triangle inequality and because  $|L_l[(X - x_0)^i (Y - y_0)^j]| \leq h^{i+j}$ . So,

$$h^n \sum_{i+j=n} |a_{i,j}| \geq \sum_{i+j=n} \left| \frac{\det(R_{00} \dots V_{ij} \dots R_{0n})}{\phi_{i,j}} \right|.$$

The left hand side of this inequality is a continuous and homogeneous of degree zero function on  $\mathcal{C}$  and hence reaches its minimum. This minimum cannot be zero because that would mean that all of the  $a_{i,j}$ 's are zero which is absurd by assumption, and is also independent of  $h$  (because of the homogeneity property).

Now let us turn to the second inequality. We have

$$h^n \sum_{i+j=n} |a_{i,j}| = \sum_{i+j=n} |\psi_{i,j}|.$$

The left hand side is also a continuous function on  $\mathcal{C}$  and is bounded above. Clearly, the latter constant does not depend on  $\epsilon$ . •

**Corollar 1.4.8** *With the assumptions of lemma 1.4.7, let  $n$  and  $p$  be integers satisfying  $p < n$ . Choose  $l$  and  $l'$  such that  $N(p-1) < l' \leq N(p)$  and  $N(n-1) < l \leq N(n)$ . Then there exist two constants  $C_1$  and  $C_2$  such that*

$$C_2(n) h^{-n+p} \geq \sum_{l, \text{card}(l)=p} |\lambda_l^{l'}| \geq C_1(n, \epsilon) h^{-n+p},$$

for any subset of cardinality  $p$ .

**Proof :** We apply the definition of  $\lambda_I^{l'}$  and the same techniques as used in the previous lemma •

Now, we may state our main result :

**Theorem 1.4.9** *Let  $S^{(n)}$  be a stencil satisfying the assumption of Lemma 1.4.7, and for some  $\epsilon_0 > 0$  the property 1.4.5. Let us also assume that the following condition, for some  $0 < \alpha \leq 1$*

$$\text{Min} \left\{ x_0 \in K, \left| \det \left[ \frac{R_{0 \ 0}}{\|R_{0 \ 0}\|} \cdots \frac{R_{0 \ n}}{\|R_{0 \ n}\|} \right] \right| \right\} > \alpha, \quad (1.16)$$

*Let  $u$  a real function defined on an open subset of  $\Omega$  in  $\mathbb{R}^2$  being  $C^1$  except perhaps on a locally  $C^1$  curve where its  $n$ -th order derivative may have a jump  $[D^n u]$  such that the intersection  $I$  of that curve and the convex hull of  $S^{(n)}$  is not empty. Then there exists a constant  $C(n, \epsilon_0, \alpha) > 0$  such that the coefficients in the Taylor expansion towards a point of  $I$  satisfy :*

$$\sum_{i+j=n} |a_{i \ j}| \geq C(n, \epsilon_0, \alpha) \frac{[D^n u]}{h^n}. \quad (1.17)$$

**Remark :** In the case of the Lagrange interpolation, for  $n=1$ , the condition (1.16) just says that the smallest angle of the triangle is not too small.

**Proof :**

Let  $u$  be a real valued function that admits continuous derivative up to order  $p-1$  and a jump in its  $p^{\text{th}}$  derivative across a locally  $C^1$  curve.  $C$ . Let us remind the recurrence relation of lemma 1.3.1 :

$$a_l^{(n)} = \sum_{l', \text{card}(l)=p} \lambda_I^{l' l} a_{l'}^{(p)}$$

where the subscript  $l$  (resp.  $l'$ ) corresponds to  $(i, j)$  with  $i+j=n$  (resp.  $i+j=p$ ) in the lexicographic ordering.

For the sake of simplicity, we assume that the curve  $C$  divides  $K$  in two parts,  $K^+$  and  $K^-$ , each of them being on one side of  $C$ . Let  $(x_0, y_0)$  be a point of  $K$ , say in  $K^+$ . We establish first the proof of the theorem for the Lagrange interpolation and show at the end of it how to adapt it for the approximation in the mean. The Taylor formula gives, for  $a \in S^{(n)} \cup K^+$  :

$$\begin{aligned} u(a) &= \sum_{l=0}^{p-1} \frac{1}{l!} \sum_{i+j=l} D_{ij} u(x_0, y_0) (a_x - x_0)^i (a_y - y_0)^j \\ &+ \frac{1}{p!} \sum_{i+j=p} D_{ij} u(\nu(x_0, y-0)) (a_x - x_0)^i (a_y - y_0)^j \end{aligned}$$

where  $\nu(x_0, y_0)$  stands for  $(\nu x_0 + (1-\nu)a_x, \nu y_0 + (1-\nu)a_y)$  for some  $\nu \in [0, 1]$ ,  $D_{ij} u(\nu(x_0, y_0)) \longrightarrow D_{ij}^+$ .

For a point of  $S^{(n)} \cap K^+$ , one gets :

$$u(a) = \sum_{l=0}^{p-1} \frac{1}{l!} \sum_{i+j=l} D_{ij} u(x_0, y_0) (a_x - x_0)^i (a_y - y_0)^j + \frac{1}{p!} \sum_{i+j=p} A_{ij} (a_x - x_0)^i (a_y - y_0)^j \quad (1.18)$$

where  $A_{ij} \rightarrow D_{ij}^-$ . In order to get this result, one has to consider, on the straight line  $[(x_0, y_0), a]$ , the function  $v$  defined by :

- if  $x \in [(x_0, y_0), a]$  is between  $(x_0, y_0)$  and  $x_C = [(x_0, y_0), a] \cap C$ ,  $v = u$ ,
- if  $x \in [(x_0, y_0), a]$  is between  $x_C$  and  $a$ ,

$$v = u + \frac{1}{p!} \sum_{i+j=p} [D_{ij}] (x - x_0)^i (y - y_0)^j$$

where  $[D_{ij}]$  represents the jump of  $D_{ij}u$  at  $x_C$ .

This function admits a continuous  $p^{\text{th}}$  derivative over  $[(x_0, y_0), a]$ , so one obtains the result 1.18.

Let  $\epsilon > 0$  be given. If the diameter of  $K$  is small enough, from these relations and the rules of evaluation of determinants, one gets :

$$a_{I'}^{(p)} = \frac{\begin{vmatrix} D_{ij}^+ L_1 [(X - x_0)^i (Y - y_0)^j] \\ \vdots \\ D_{ij}^+ L_m [(X - x_0)^i (Y - y_0)^j] \\ R_{00} \cdots D_{ij}^- L_{m+1} [(X - x_0)^i (Y - y_0)^j] \cdots R_{0p} \\ \vdots \\ D_{ij}^- L_{N(p)} [(X - x_0)^i (Y - y_0)^j] \end{vmatrix}}{\det(R_{00} \cdots R_{0p})} \quad (1.19)$$

$$+ \frac{\begin{vmatrix} o(1) L_1 [(X - x_0)^i (Y - y_0)^j] \\ \vdots \\ o(1) L_m [(X - x_0)^i (Y - y_0)^j] \\ R_{00} \cdots o(1) L_{m+1} [(X - x_0)^i (Y - y_0)^j] \cdots R_{0p} \\ \vdots \\ o(1) L_{N(p)} [(X - x_0)^i (Y - y_0)^j] \end{vmatrix}}{\det(R_{00} \cdots R_{0p})},$$

where the index  $I'$  stands for  $(i, j)$  in the lexicographic order,  $L_i(u) = u(a_i)$  and  $|o(1)| \leq \epsilon$ .

For the sake of simplicity, let us denote by  $\mu_I$  and  $\nu_I$  the coefficients obtained from the first part of the right hand side of equation 1.19 by replacing  $D_{ij}^+$  by 1 and  $D_{ij}^-$  by 0 for  $\mu_I$  and vice versa for  $\nu_I$  so that

$$a_{I'}^{(p)} = (D_{ij}^+ + o(1)) \mu_I + (D_{ij}^- + o(1)) \nu_I.$$

We have to notice that the sum of  $\mu_I$  and  $\nu_I$  is one, and that if all the points of  $I$  are on the same side of  $C$ , then either  $\mu_I$  or  $\nu_I$  is zero. Then, using lemma 1.3.2 and the above remarks, we have :

$$a_I^{(n)} = [D_{ij}] \sum_{\text{card}(I)=p} \nu_I \lambda_I^{I'} + \sum_{\text{card}(I)=p} o(1) \mu_I \lambda_I^{I'} + \sum_{\text{card}(I)=p} o(1) \nu_I \lambda_I^{I'},$$



so that

$$||D_{ij}|| \underbrace{h^{p-n} \left| \sum_{\substack{card(I)=p \\ I}} \nu_I \lambda_I^{l'} \right|}_I \leq h^{p-n} |a_i| + \underbrace{\epsilon h^{p-n} \sum_{\substack{card(I)=p \\ II}} (|\mu_I| + |\nu_I|) |\lambda_I^{l'}|}_{II}. \quad (1.20)$$

Because of inequality (1.16) and from Hadamard's inequality, one has :

$$|\mu_I| + |\nu_I| \leq \frac{\sqrt{\sum_{a \in S_+} L_a [(X - x_0)^i (Y - y_0)^j]^2} + \sqrt{\sum_{a \in S_-} L_a [(X - x_0)^i (Y - y_0)^j]^2}}{\alpha ||R_{q'}||}.$$

(Note that we have identify the point of the point  $a$  and its index in the ordering.) This latter expression is bounded above by a constant  $C_0$  because  $l'$  corresponds to  $(i, j)$  in the lexicographic order, without any additional conditions on the geometry and because  $L_a$  is continuous. With the help of lemma 1.3.2, the expression  $II$  of (1.20) is bounded above by a constant  $C_1$ .

The term  $I$  of (1.20), with the help of lemma 1.3.1 can be seen as the  $l^h$  coefficient of a polynomial that admits the values  $L_a [(X - x_0)^i (Y - y_0)^j]$  where  $a \in K^-$ . At least one of these value is not zero because the curve  $C$  cuts  $K$  so that there are points of  $S^{(n)}$  on both sides of  $C$  and  $(x_0, y_0) \in K^+$ . When summing up these equalities for  $i + j = n$ , the same proof as in lemma 1.3.1 shows that this expression is bounded above by a constant  $C_2 \neq 0$ . Then, one gets our result for  $\epsilon$  small enough.

In the case of the approximation of the mean, the same kind of arguments may be applied because :

- if  $C_a \subset K^+$  or  $K^-$ , these exist  $\alpha_a \in C_a$  such that

$$< u >_{C_i} = u(\alpha_a)$$

- if  $C_a$  cuts  $C$ , then there exists  $\alpha_a^+ \in C_a \cap K^+$  and  $\alpha_a^- \in C_a \cap K^-$  such that :

$$< u >_{C_i} = \frac{\text{aire}(C_a \cap K^+)}{\text{aire}(C_a)} u(\alpha_a^+) + \frac{\text{aire}(C_a \cap K^-)}{\text{aire}(C_a)} u(\alpha_a^-). \quad \bullet$$

This result enables us to detect the regions of smoothness from those where a jump in one of the derivatives occurs.

## Chapter 2

# An E.N.O. Reconstruction Technique

In recent papers, Harten and several other authors [3,4,5,6,7] have tried to derive numerical methods that are able to achieve a higher order of accuracy than classical TVD methods. There are several versions of these techniques, but they can be generally viewed in the following way : starting from some approximation of a real function  $u$  (point values or average values in some control volumes), find a pointwise high order approximation  $u$ . Two tools are then used :

- an essentially non oscillatory Lagrange interpolation of a function  $w$ ,
- this function  $w$  may be  $u$  itself if one starts from point values or either the primitive function of  $u$  or its convolution product with the characteristic function of a copy of the control volume if one can pass from one to another by a translation.

The latter deconvolution technique can only be applied, at least in its standard version, to regular meshes as shown in section 2.2.1.

In this section, we want to adapt both tools to the situation of unstructured meshes. At least for the second point, the situation seems at first glance very bad : the reconstruction via primitive function cannot be applied in the case of unstructured meshes because the only solution would be to apply it to integrals over domains like  $\mathcal{D}_M = [a_1, b_1] \times [a_2, b_2]$ , possibly with a suitable transformation of the plane as in [9], which are not in general the union of control volumes.

Now, the reconstruction via deconvolution technique can only be applied to regular meshes (i.e. meshes where the control volumes are translated from one node to another). In this section, we show how to adapt this technique for irregular meshes.

In what follows,  $\mathcal{T}$  is a triangulation of  $\Omega$ , a domain of  $\mathbb{R}^2$ ,  $u$  is a function defined on that domain. Around each node  $i$  of  $\mathcal{T}$ , we may define a control volume  $C_i$  in many different ways. An example is (see Figure 2.2) the control volume whose boundary is the segment joining the centroids  $G$  of the triangles  $(i, j, k)$  having  $i$  as a vertex and the middles  $I_1, I_2$  of the segments of those triangles (type I). Another type of control volume is obtained by

considering each triangle as the control volume of its centroid. The triangulation we need to describe the ENO algorithm is not  $\mathcal{T}$  but another one built from the centroids of the triangles of  $\mathcal{T}$ .

## 2.1 Non oscillatory interpolation

Let us consider  $n > 0$ . In this section, we show how to generalize the  $n + 1$ -th order E.N.O. interpolation technique exposed in [4,5] to unstructured meshes. As the results of chapter 1 indicate it, we must deal with meshes where the stencils we need satisfy the property of theorems 1.4.1 and 1.4.9. This will be the case for most meshes.

Let  $\mathcal{T}$  be a triangulation of  $\Omega$ , a domain in  $\mathbb{R}^2$ , and  $u$  a function defined on that domain. The results we have obtained in chapter 1 can be summarized as follows :

- if  $\mathcal{S}^{(n)}$  is an admissible stencil such that  $u$  is smooth in its convex hull, then

$$\sum_{i+j=n} |a_{i,j}|,$$

remains finite,

- if in the convex hull of  $\mathcal{S}^{(n)}$ ,  $u$  admits continuously differentiable derivatives only up to the order  $k < n$ , then

$$\sum_{i+j=n} |a_{i,j}| = O([u^{(n)}] h^{k-n}),$$

where  $h$  is the diameter of  $\mathcal{S}^{(n)}$ .

Then, as suggested by [4,5], the E.N.O. algorithm we propose is to consider  $\Pi_1(u)$  defined on  $C_i$  by the following recursive algorithm :

For a node  $i$ ,

1. Let  $\{T_i\}$  be the set of triangles of  $\mathcal{T}$  having  $i$  as a vertex. Consider all the linear interpolations where the  $T_i$ 's are the stencils. Choose the one,  $T_{min}$ , where the sum

$$\sum_{i+j=1} |a_{i,j}|,$$

is minimal. We set  $\mathcal{S}^{(1)} =$  the nodes of  $T_{min}$ .

2. Let  $\mathcal{S}^{(n-1)}$  be the stencils defined at the previous step. Consider all the nodes surrounding  $\mathcal{S}^{(n-1)}$  in  $\mathcal{T}$  and consider all the stencils obtained from  $\mathcal{S}^{(n-1)}$  by adding  $n + 1$  of the nodes surrounding  $\mathcal{S}^{(n-1)}$ . Choose the stencil minimizing :

$$\sum_{i+j=n} |a_{i,j}|.$$

We have intentionally left the second point imprecise because it is obvious that the number of stencils to consider is in general huge. To give an example, if one considers Figure 2.3 for which  $n = 2$ , one sees that possible stencils are the vertices of triangles  $T_{min}$  and 3 of the ten other triangles. This can be repeated for each of the three edges of  $T_{min}$  and leads to a total of  $3 \times C_{10}^3 = 360$  possible stencils ! So, one has to define criteria for choosing the "good" and "bad" stencils. These criteria are essentially heuristic and *a priori* ones .

One that seems natural is that when one considers the control volume around each node, the collection of the control volumes of all points of the stencil should be convex. Another one is that the criteria leads to the smallest possible number of stencils, but the stencils must not be confined in a particular angular area of the plane, in order not to favor any direction.

With this in mind, two possible sets of stencils for third order interpolation are (see Figure 2.3) :

- the nodes of triangle  $T_{min}$  plus, for each of its edges, the three additional nodes of triangles  $T_1, T_2, T_3$ . This leads to a maximum of three stencils per triangle,
- or the nodes of triangles of  $T_{min}$  plus, for each of its edges, the three additional nodes of triangles of
  - $T_1, T_2, T_3$ ,
  - $T_1, T_2$  and  $T_4$  or  $T_5$ ,
  - $T_1, T_3$  and  $T_6$  or  $T_7$ ,
  - $T_1, T_9$  or  $T_{10}$  and one of the six triangles  $T_2, T_3, T_4, T_5, T_6, T_7$ .

The second solution leads to a maximum number of 52 stencils once  $T_{min}$  has been found. We have made several tests to evaluate the "performance" of each type of stencil. They are given in section 3 and indicate that the first kind of stencil is sufficient.

These experimental results suggests the following algorithm for selecting stencils for higher order of accuracy (of course, in this case, the problem of choosing the smallest number of possible stencils is much more critical than for third order interpolation !).

To begin with, we notice that the six points of  $T_{min}$ ,  $T_1$ ,  $T_2$  and  $T_3$ , denoted by  $\mathcal{S}^{(3)}$  in the sequel, form a set isomorphic to the standard stencil for  $P_2$  interpolation (see Figure 2.4). Now, this stencil can be embedded in the standard stencil for  $P_3$  interpolation (Figure 2.4) where the additional points 7,8,9,10 are the new points introduced for 4<sup>th</sup> approximation.

Let us consider a "side" of  $\mathcal{S}^{(3)}$ , say the points 4,5,6. Since the mesh is conformal, the segment 4-5 is the edge of two triangles in general,  $T_1$  and a new one,  $T_4$ . The same is true for the segment 5-6 and a new triangle  $T_5$  is introduced. Then the sides of these new triangles are the edge of some triangle,  $T_6$  and possibly  $T_8$  for  $T_4$ . So, at most four new triangles,  $T_6, T_7, T_8, T_9$  are introduced and the new stencils are made of  $\mathcal{S}^{(3)}$  and the points of  $\{T_4, T_6, T_8, T_5\}$  or  $\{T_4, T_5, T_9, T_7\}$  or  $\{T_4, T_8, T_9, T_5\}$  when  $T_8 \neq T_9$ . These two or three new stencils are isomorphic to the standard  $P_3$  stencil as shown on Figure 2.4. These new procedure may be repeated for the three sides of  $\mathcal{S}^{(3)}$  and so at most 12 stencils must be considered for  $\mathcal{S}^{(3)}$ .

By using the similarity between  $\mathcal{S}^{(n)}$  and the standard stencil for  $P_n$  interpolation, induction can easily be applied to construct a small, but probably sufficient, set of stencils  $\mathcal{S}^{(n+1)}$

This particular interpolation is  $n + 1$ -th order accurate; because  $u$  is a polynomial of degree less than  $n$ , we have  $\Pi_1(u) = u$ . This property ensures the  $n + 1$ -th order accuracy [16], and in particular, we have the estimations of theorem 1.4.1.

## 2.2 Two conservative ENO reconstruction

Two kinds of reconstructions are now considered. A first one inspired from the so-called reconstruction technique and a second one, already considered by Harten et al. without rigorous justification in a very recent paper [8].

### 2.2.1 Deconvolution technique revisited

If  $(x)_{i \in \mathbb{N}}$  is a regular mesh of  $R$  and  $u$  is a real valued function on  $\mathbb{R}$ , the reconstruction by the deconvolution technique consists of applying the previous algorithm, not to  $u$  but to

$$\bar{u}_i(y) = \frac{1}{x_{i+1} - x_i} \int_{x_{i-1/2}}^{x_{i+1/2}} u(x + y - x_i) dx, \quad (2.1)$$

where, as usual, the mesh size  $\Delta x = x_{i+1} - x_i$  is constant and  $x_{i+1/2} = x_i + \Delta x/2$ . In particular, we see that  $\bar{u}_i$  does not depend on  $i$  and that  $\bar{u}(x_i)$  is the average of  $u$  on  $[x_{i-1/2}, x_{i+1/2}]$ . These values are assumed to be known. Let  $\Pi_1(\bar{u})$  be the  $m + 1$ -th order Lagrange interpolation as described in the previous section, with  $m \geq n$ . Then, the idea is to perform a Taylor expansion of  $\bar{u}$  and its successive derivatives around  $x_i$ , to truncate them at order  $n - k$ , to replace the values  $\bar{u}, \dots, \bar{u}^{(n)}$  by  $\Pi_1(\bar{u})$  and its  $n$  successive derivatives, and to replace the values of  $u$  by those of  $\Pi_2(u)$ , the approximation of  $u$  we are looking for :

$$\begin{aligned} \Pi_1(\bar{u})(x_i) &= \sum_{l=1}^n \alpha_i^l \frac{\Pi_2(u)^{(l)}(x_i)}{l!}, \\ &\vdots \\ \Pi_1(\bar{u})^{(k)}(x_i) &= \sum_{l=1}^{n-k} \alpha_i^l \frac{\Pi_2(u)^{(l+k)}(x_i)}{l!}, \\ &\vdots \\ \Pi_1(\bar{u})^{(n)}(x_i) &= \alpha_i^n \frac{\Pi_2(u)^{(n)}(x_i)}{n!}, \end{aligned} \quad (2.2)$$

where

$$\alpha_i^l = \frac{\int_{x_{i-1/2}}^{x_{i+1/2}} (x - x_i)^l dx}{\Delta x}.$$

The linear system is easily invertible because the matrix is upper triangular and its diagonal consists of all “1”s. Furthermore, it is shown in [4], for example, that the average value of

$\Pi_2(u)$  over  $[x_{i-1/2}, x_{i+1/2}]$  is exactly  $\bar{u}_i$ . Last, this approximation has the desired order of accuracy when  $u$  is smooth because polynomials are left invariant by the construction.

This latter point is the fundamental reason why one achieves the expected order of accuracy. Polynomials are left invariant by the construction because the shape of the control cells does not change from one point to another. If this were not the case, i.e if  $\Delta x_{i+1/2} = x_{i+1} - x_i$  were not constant, the formula (2.1) would indeed depend on the point  $x_i$  and this property would be lost. In order to show this, we simply consider  $u(x) = x$  and a  $m + 1$ -th order interpolation that has values  $\bar{u}_i$  at points  $x_i$ . Assuming that  $\{x_0, x_1, \dots\}$  is the stencil selected by the E.N.O. algorithm, we have :

$$\Pi_1(\bar{u}) = \bar{u}_0 + K(x - x_0) + \dots \quad \text{where} \quad K = \frac{1}{2} + \frac{\Delta x_{3/2} + \Delta x_{-1/2}}{\Delta x_{1/2}}.$$

When the mesh is not regular,  $K \neq 1$  in general. To obtain  $\Pi_2(u) = u$ , one must have :

$$\begin{aligned} \Pi_1(\bar{u})(y) &= u(y) + \alpha_1 u'(y), \\ \Pi_2(\bar{u})'(y) &= K = u'(y). \end{aligned}$$

The second equation indicates that one must have  $K = 1$  which is, in general, not true.

To overcome this problem, we propose the following technique : apply the ENO search algorithm not to  $\bar{u}$  defined by equation 2.1 but to :

$$\bar{u}(y) = \frac{1}{\text{area}(C_{S^{(n)}})} \int_{C_{S^{(n)}}} u(x + y - x_0) dx, \quad (2.3)$$

where  $S^{(n)}$  is any possible stencil around the node  $x_0$  that one has to test and  $C_{S^{(n)}}$  is the union of the control volumes of each node in  $S^{(n)}$  :

$$C_{S^{(n)}} = \bigcup_{j \in S^{(n)}} C_j. \quad (2.4)$$

Now, one has to evaluate the integral (2.3) from the average value of  $u$ . This cannot generally be achieved for any function, but is possible for the polynomials of  $\mathbb{R}_n[X, Y]$ , at least in general. This will be true for the  $N(n)$  linear forms over  $\mathbb{R}_n[X, Y]$  when

$$\langle P \rangle_{C_i} = \frac{1}{\text{area} C_i} \int_{C_i} P(x) dx, \quad \text{for all } P \in \mathbb{R}_n[X, Y], \quad (2.5)$$

are independent. For all the meshes we have considered, these linear forms were always independent, so the problem had a solution. If this is true, then one can find coefficients  $\alpha_l(y)$ ,  $1 \leq l \leq N(n)$  so that

$$\frac{1}{\text{area}(C_{S^{(n)}})} \int_{C_{S^{(n)}}} u(x + y - x_0) dy = \sum_{l=1}^{N(n)} \alpha_l(y) \langle u \rangle_{C_i}, \quad (2.6)$$

when  $u$  belongs to  $\mathbb{R}_n[X, Y]$ . If not, the equation (2.6) gives a  $n + 1$ -th order quadrature formula. With all this, we get the following theorem whose proof is obvious.

**Theorem 2.2.1** *The algorithm defined by the E.N.O. technique with (2.3), (2.4), (2.5) and (2.6) leaves invariant the polynomials of  $\mathbb{R}_n[X, Y]$  and hence gives a  $n + 1$ -th order approximation of smooth functions. Moreover, this approximation is conservative up to the quadrature formula (2.6).*

## 2.2.2 A formally conservative reconstruction

A second reconstruction technique, which is formally conservative, may be the following : as noticed in theorems 1.4.1 and 1.4.9, the regions of smoothness of a function  $u$  may be detected from the behaviour of the highest order coefficients of the approximation in the mean  $\Pi_M(u)$  for all the possible stencils surrounding a given node  $i$ . The reconstruction we consider is the defined by the polynomial having the lower highest order coefficients because, as in the previous section, the results of chapter may be summarised as follow for the approximation in the mean :

- if  $S^{(n)}$  is an admissible stencil such that  $u$  is smooth in its convex hull, then

$$\sum_{i+j=n} |a_{i,j}|,$$

remains finite,

- if in the convex hull of  $S^{(n)}$ ,  $u$  admits continuously differentiable derivatives only up to the order  $k < n$ , then

$$\sum_{i+j=n} |a_{i,j}| = O([u^{(n)}] h^{k-n}),$$

where  $h$  is the diameter of  $S^{(n)}$ .

Then exactly the same algorithm as before may be applied in order to select the “smoothest” stencil for the approximation around a given node. Since this node always belongs to any possible stencil, then the reconstruction is conservative from the definition of  $\Pi_M$ . For the same reasons than in the previous paragraph, the same accuracy properties are also true, and the constant of theorem 1.4.1 is the supremum of all the  $C(n, S^{(n)'})$  for all the stencils considered in the reconstruction.

In practice, the set of possible stencils is defined by induction from the algorithm we propose in paragraph 2.1.

## 2.3 Some remarks for the practical calculation of the reconstruction

In section 1.2.1, we have discussed the problem of the practical determination of the coefficients of a Lagrange interpolant because the linear systems to be solved have in general small coefficients. The same problem also arises here if one uses the monomials  $(X - x_0)^i (Y - y_0)^j$  to

determine the  $\alpha_l(y)$  of equation 2.6. This can easily be seen by using Hadamard's inequality as in section 1.2.1.

For a given node  $x_0$ , the E.N.O. technique we propose naturally introduces one triangle having that node as vertex, the triangle  $T_{min}$  as in Figure 2.3 . So, as in section 1.2.1, we will use the barycentric coordinates towards that triangle for practical computations.



# Chapter 3

## Numerical examples

We have performed several tests on the second, third and fourth order E.N.O. interpolation and E.N.O. reconstruction, but we only report the third and fourth order results since they are *a priori* more challenging. In particular, we intend to check numerically that the expected order of accuracy is in fact reached for smooth functions.

In all these examples, we have assumed that the control volumes are of "type I". The practical calculations of the averages in these control volumes have been performed with a 5-th order quadrature formula [15].

The tests on smooth functions are performed on :

$$u(x, y) = \cos(2\pi(x^2 + y^2)).$$

The mesh size  $h$  has been measured by choosing the largest segment of the triangulation. All the error estimates have been obtained on irregular meshes as the one presented on Figure 3.5. These meshes are obtained as random perturbations of regular structured meshes. The set of points that one obtains is triangulated by the Bowyer algorithm to get a Delaunay triangulation. The main difference between such a mesh and the regular structured one is that the number of triangles each node belongs to is different. We also have done the same tests with regular meshes, and we have not seen any degradation of the convergence.

The locally smooth function we have chosen is obtained by a modification of that used by Harten in [7] for example : if  $\phi$  is any angle, let  $f_\phi$  be :

$$f_\phi(x, y) = \begin{cases} \text{if } r \leq -\frac{1}{3}, & f_\phi(x, y) = -r \sin\left(\frac{\pi}{2}r^2\right), \\ \text{if } r \geq \frac{1}{3}, & f_\phi(x, y) = 2r - \frac{1}{6} \sin(3\pi r), \\ \text{if } |r| < \frac{1}{3}, & f_\phi(x, y) = |\sin(2\pi r)|, \end{cases} \quad \text{where } r = x + \tan(\phi)y, \quad (3.1)$$

and let  $u$  be :

$$\begin{cases} \text{if } x \leq \frac{1}{2} \cos \pi y, & u(x, y) = f_{\sqrt{\pi/2}}(x, y), \\ \text{if } x > \frac{1}{2} \cos \pi y, & u(x, y) = f_{-\sqrt{\pi/2}}(x, y) + \cos(2\pi y). \end{cases} \quad (3.2)$$

The function defined by (3.1)-(3.2) shows discontinuities in the function itself and its first order derivatives; some of the discontinuities are straight lines (never aligned to the mesh), one is a curved line where the jump changes from one point to another. Last, the behaviour of  $u$  is basically one-dimensional on the left of the curve  $x = \cos \pi y/2$  and really two-dimensional on the right.

A plot of this function is given in Figure 3.6. One should obtain straight lines and smooth discontinuity transitions contrary to what is shown in the Figure : this is an effect of the graphic device adapted to  $P_1$  interpolation.

**Third order interpolation and reconstruction** No visible difference can be seen between the two kind of reconstructions (directly from mean values and by deconvolution), except on the cost of each algorithm. Because of that, most of the results are presented from the “reconstruction on the mean” technique except if specified.

The two types of stencils (as presented in section 2.1 ) have been tested in this case. The use of the second type of possible stencils results in a much more expensive approximation (in general, one must test 52 stencils per triangle versus only 3 in the simplest version) and the results have never been dramatically improved. All the results that are presented bellow have been obtained with the 3 stencil version of the method.

We have displayed in Figure 3.7 the  $L^\infty$  error of the interpolation for the smooth test case. The plain curve with squares is obtained with the E.N.O. interpolation, the plain curve with circles is obtained with the E.N.O. reconstruction. The dashed line indicates the slope  $-3$ . One can see that the expected order of accuracy is indeed reached.

In Figures 3.9-(a) and 3.10-(a), we have displayed the node values of the E.N.O. reconstruction for two meshes (1600 nodes and 6400 nodes). To better see the behaviour of both approximation techniques, we also present cross-section on three lines :  $Y = 0.75$ ,  $Y = 0$  and  $Y = -0.45$  (Figures 3.12, 3.13 and 3.14. The approximations are obtained from the 1600 nodes mesh (see Figure 3.5) by the deconvolution technique. The latter line goes through one of the triple points (see Figure 3.6). One can see that the various discontinuities and the smooth regions are well captured by both techniques.

The Figure 3.11 represents the overall values of the reconstructed function by deconvolution and can be compared to Figure 3.10-(a).

**Fourth order interpolation and reconstruction** The same tests have been performed for the fourth order interpolation and reconstruction of the smooth function. The Figure 3.8 shows the  $L^\infty$  error of the ENO reconstruction for random meshes. The Figures 3.9-(a) and 3.10-(b) shows an overall picture of the fourth order ENO reconstruction. A better capture of the area surrounding the triple points is the only visible difference between third and fourth order reconstruction.

To end this section, we must note that the algorithm for choosing the stencils may lead to some difficulties at the boundaries as can be seen in Figure 3.6 on the left upper corner :

the most left upper triangle of the mesh (Figure 3.5) does not admit any additional points of the type we consider to make a stencil.

# Conclusion

In this report, we have developed and analyzed three methods for the reconstruction of a function admitting discontinuities only on regular planar curves from their node values or from their averages in control volumes that surround them. They are based on two polynomial approximations of real valued functions, the Lagrange interpolation and what we have called the approximation in the mean. In order to give a firm basis to the Essentially Non-Oscillatory interpolation and reconstruction, we have studied the behaviour of the highest order coefficients of these two polynomial approximations of smooth functions and unsmooth ones for which the discontinuities lie on regular curves. We have also given an adaptation of the so called "reconstruction via deconvolution" to irregular triangulated meshes. The approximation in the mean leads to a very efficient ENO reconstruction that seems to be the cheapest one. We also propose an heuristic algorithm for selecting the smallest number of possible stencils.

These techniques have been shown to work quite well on smooth and unsmooth functions. In particular, we have shown in these examples that the minimum number of possible stencils was sufficient for our purpose. We have not been able to make a rigorous study of the quality in term of convergence of these new approximation; that study is clearly needed. In a future paper, we will give application of these new approximation for deriving new algorithm for compressible Fluid Mechanics.

**Acknowledgements :** This work has been partly done under contract NAS-18605 while the author was in residence at ICASE, NASA Langley Research Center, Hampton, Virginia.

# Bibliography

- [1] H.C. Yee *Upwind and Symmetric Shock-Capturing Schemes*. Technical Report-TM-89464, NASA, May 1987.
- [2] L. Fezoui, B. Stoufflet. A Class of Implicit Upwind Schemes for Euler Simulations with Unstructured Meshes. *Journal of Computational Physics*, 84(1) pp : 174-206, September 1989.
- [3] A. Harten & S. Osher Uniformly High-Order Accurate Nonoscillatory Schemes-I, *SIAM Journal of Numerical Analysis*, Vol. 24, No 2, April 1987, pp. 279-309.
- [4] A. Harten, S. Osher, B. Engquist & S. R. Chakravarthy, Some Results on Uniformly High-Order Accurate Essentially Nonoscillatory Schemes, *Applied Numerical Analysis* 2 (1986), pp. 347-377, Elsevier Science Publishers B.V (North Holland).
- [5] A. Harten, B. Engquist, S. Osher & S. R. Chakravarthy, Uniformly High Order Accurate Essentially Non-Oscillatory Schemes III, *Journal of Computational Physics*, Vol 71, pp. 231-303. (1987).
- [6] C.W. Shu & S. Osher, Efficient Implementation of Essentially Non-Oscillatory Shock-Capturing Schemes, *Journal of Computational Physics*, Vol 77, pp.439-471 (1988).
- [7] A. Harten ENO Schemes with Subcell Resolution, *Journal of Computational Physics*, Vol 83, pp.148-184 (1989).
- [8] A. Harten & S. R. Chakravarthy, Multi-dimensional ENO Schemes for General Geometries, CAM Report 91-16, UCLA, August 1991.
- [9] J. Casper & H.L. Atkins, Finite-Volume Application of High Order ENO Schemes to Two-Dimensional Boundary-Value Problems, Submitted to the *Journal of Computational Physics*.
- [10] T. J. Barth & P.O. Frederickson, High Order Solution of the Euler Equations on Unstructured Grids using Quadratic reconstruction, AIAA Paper No 90-0013, 28 th Aerospace Science Meeting, January 8-11, Reno, Nevada.
- [11] K.C. Chung & T. H. Yao, On Lattices Admitting Unique lagrange Interpolations, *SIAM Journal of Numerical Analysis*, Vol 14, No 4, September 1977, pp. 735-743.

- [12] G. Muhlbach, The General Recurrence Relation for Divided Differences and the General Newton-Interpolation-Algorithm with Applications to Trigonometric Interpolation. *Numerische Mathematik*, Vol 32, pp. 393-408, 1979.
- [13] G. Muhlbach, The General Neville-Aitken-Algorithm and Some Applications. *Numerische Mathematik*, Vol 31, pp. 97-110, 1978.
- [14] F.R. Gantmacher, The theory of matrices, Vol I, Chelsea Publishing Compagny, New York, N.Y., 1960.
- [15] G. Strang & G. J. Fix, An analysis of the finite element method. Prentice-Hall INC., Englewood Cliffs, N.J., 1973
- [16] P.G. Ciarlet & P. A. Raviart, General Lagrange and hermite interpolation in  $\mathbb{R}^n$  with application to Finite Element Methods. *Archive for Rational Mechanics and Analysis*, Vol 42, 1972, pp. 177-199.

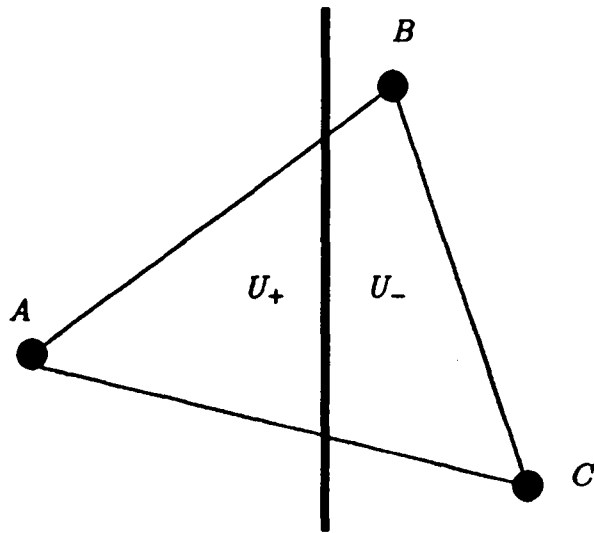


Figure 2.1: Stencil and discontinuity curve

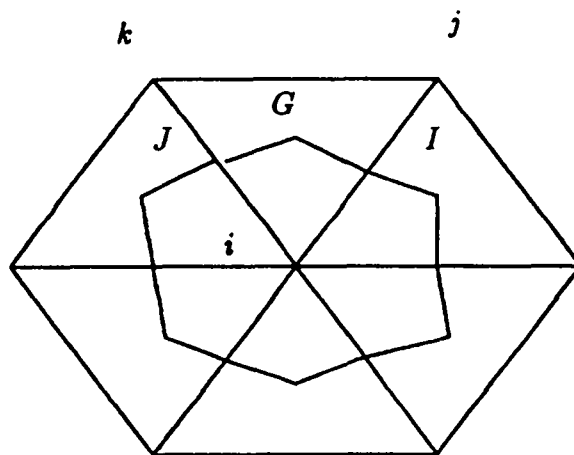


Figure 2.2: Control volume around  $i$

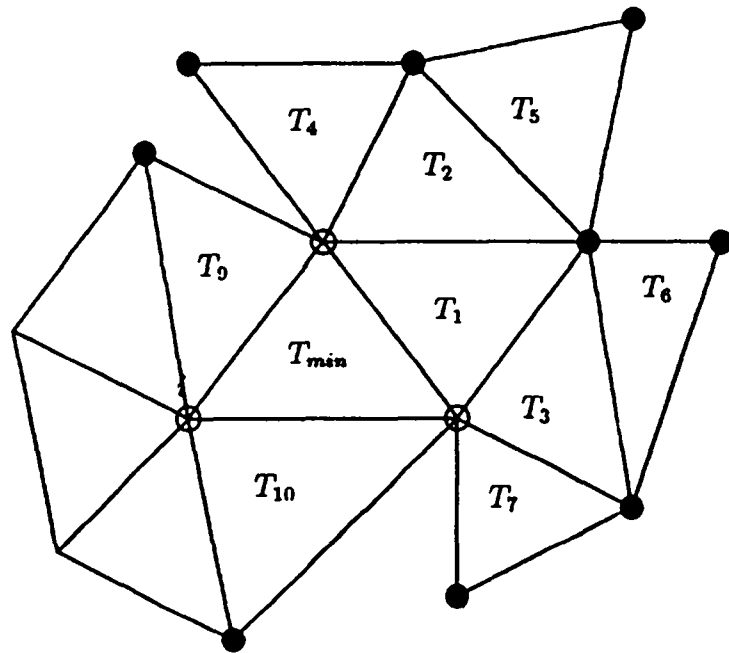


Figure 2.3: Some possible interpolation points. Circles : points of  $T_{min}$  (second order interpolation), black circles : points that may be added to obtain a stencil for third order interpolation.



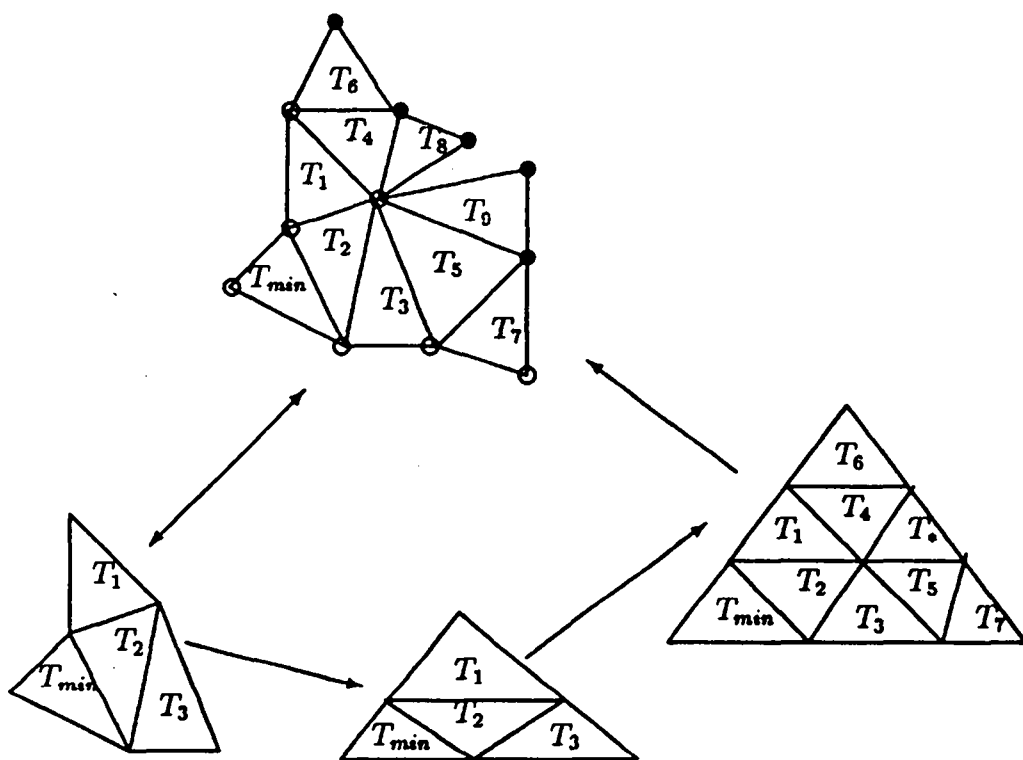


Figure 2.4: Construction of a stencil for fourth order approximation : the black circles represent the points to be added to a stencil for third order approximation (circles). The standard  $P_3$  stencil is shown.

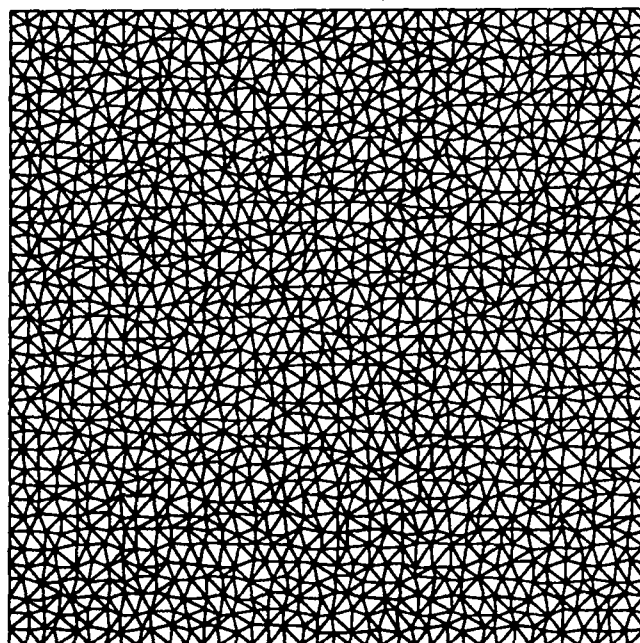


Figure 3.5: Typical mesh. 1600 nodes, 3042 triangles.

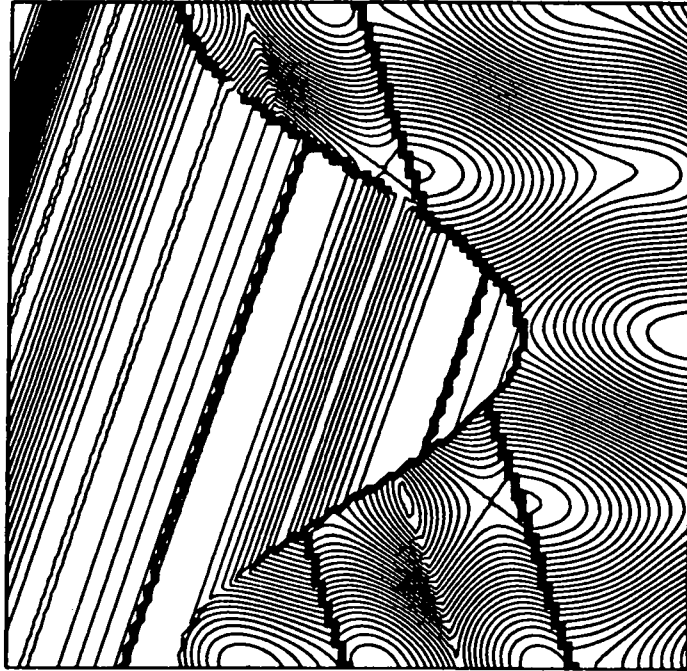


Figure 3.6: Exact function. Min=-1.331, Max=2.650,  $\delta = 0.1$ .

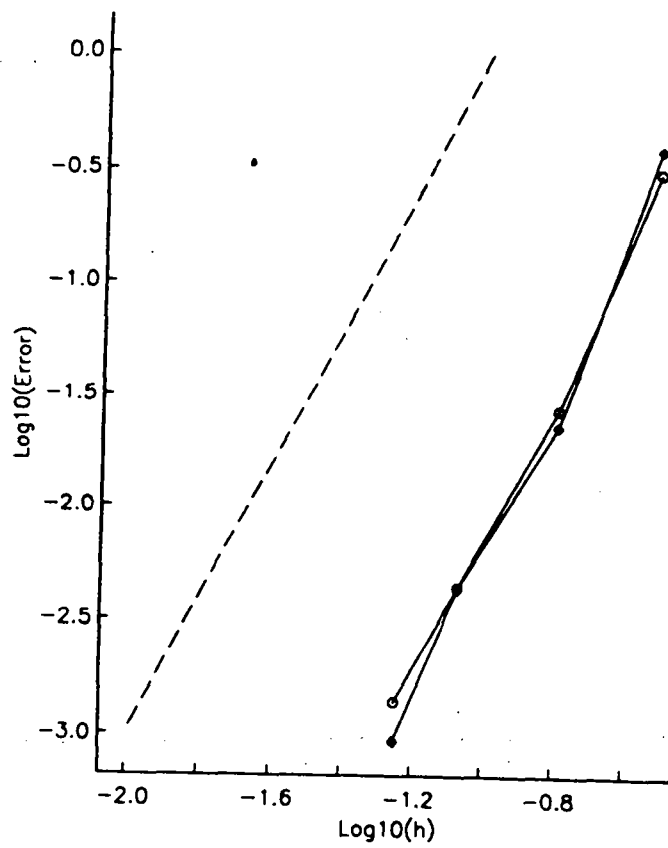


Figure 3.7:  $L^\infty$  error for  $f(x, y) = \cos[2\pi(x^2 + y^2)]$ . Squares : E.N.O. interpolation only, Circles : E.N.O. + reconstruction. Dashed line : slope -3

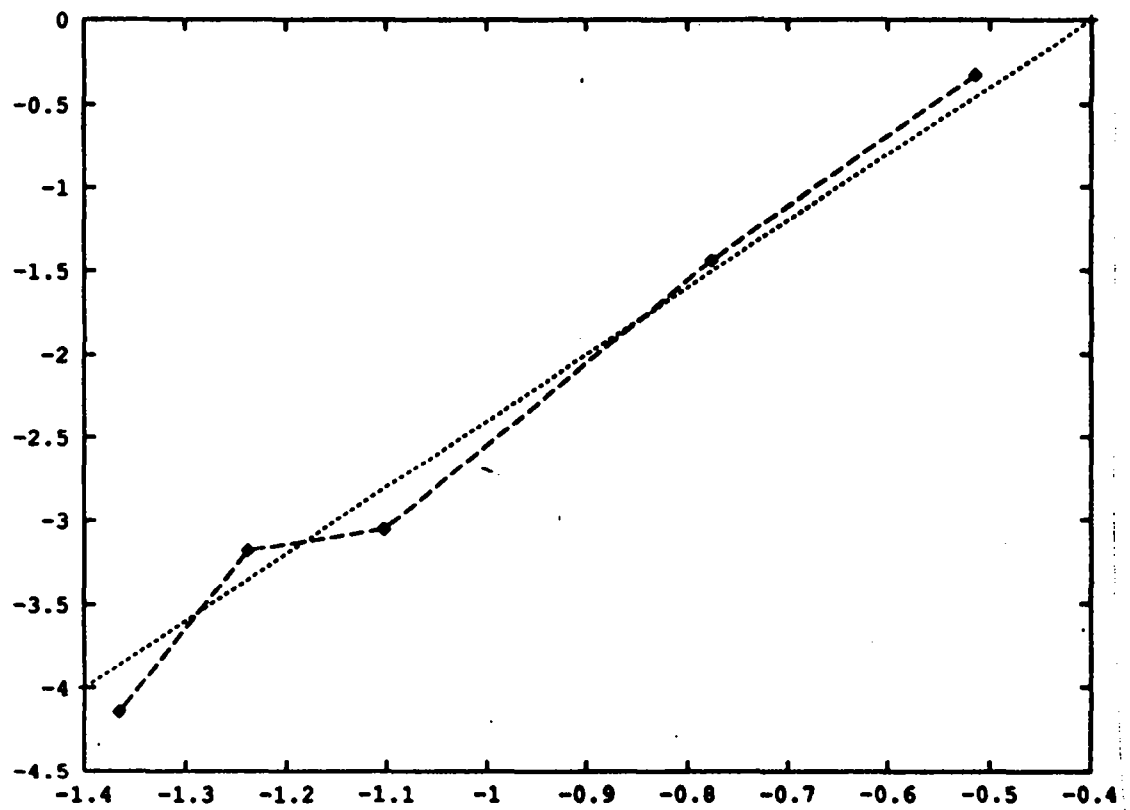
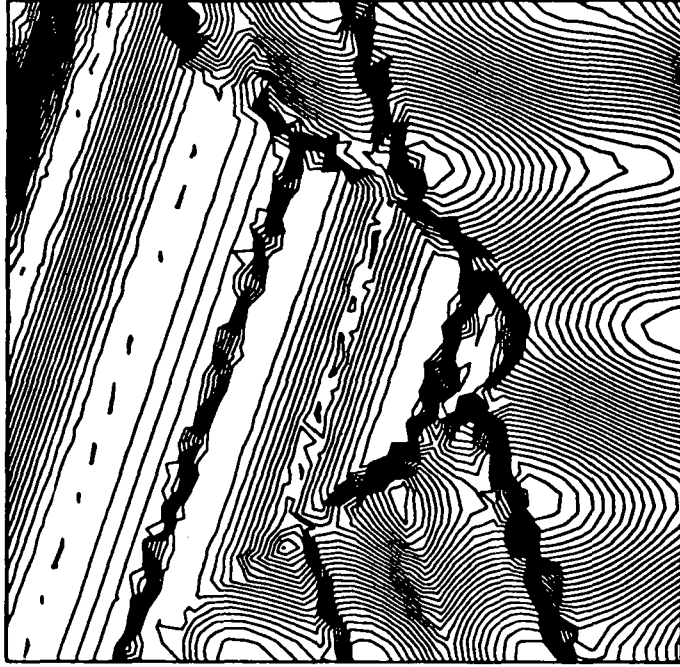


Figure 3.8:  $L^\infty$  error for  $f(x, y) = \cos[2\pi(x^2 + y^2)]$ . Squares : Dashed line : slope -4, Dashed+squares : E.N.O. + reconstruction

(a) Third order



(b) Fourth order

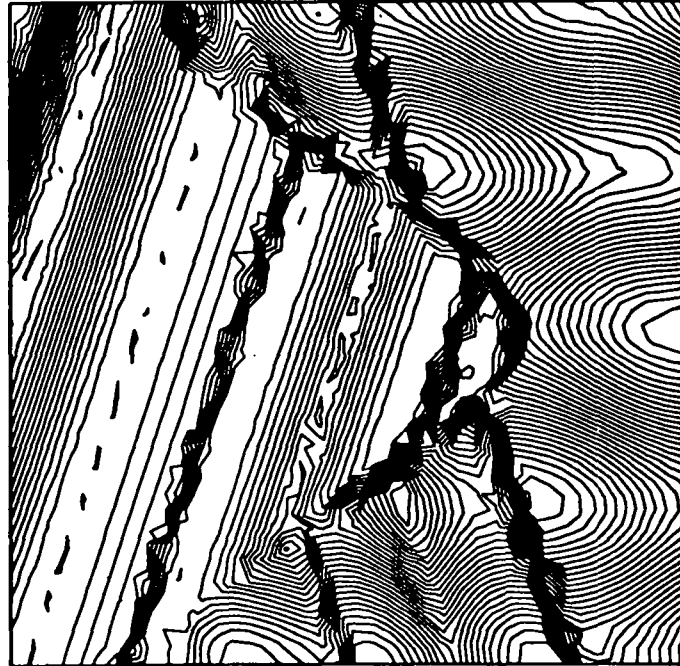


Figure 3.9: E.N.O. reconstruction “in the mean” with the 1600 nodes mesh. Min=-1.30, Max=2.6,  $\delta = 0.1$ .

(a) Third order



(b) Fourth order

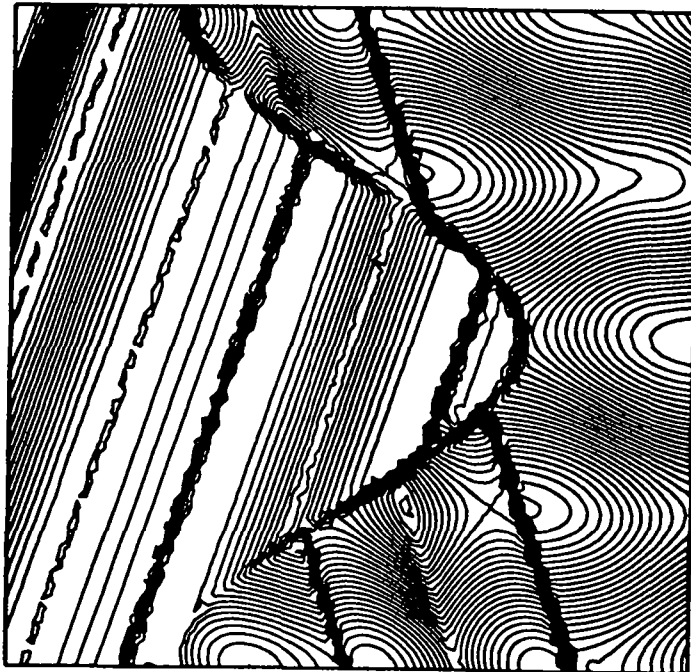


Figure 3.10: E.N.O. reconstruction “in the mean” with the 6400 nodes mesh. Min=-1.30, Max=2.6,  $\delta = 0.1$ .

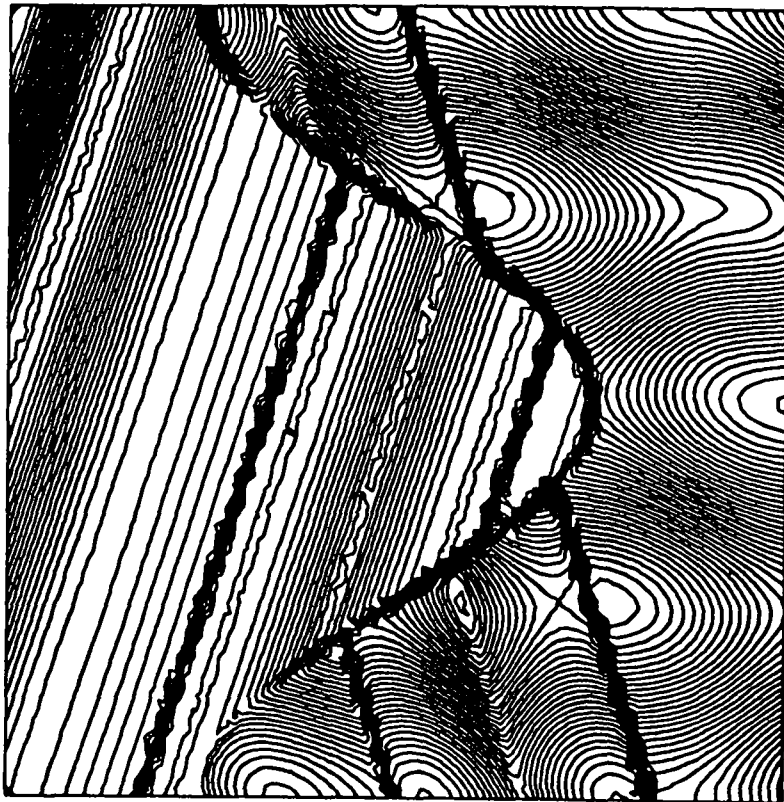
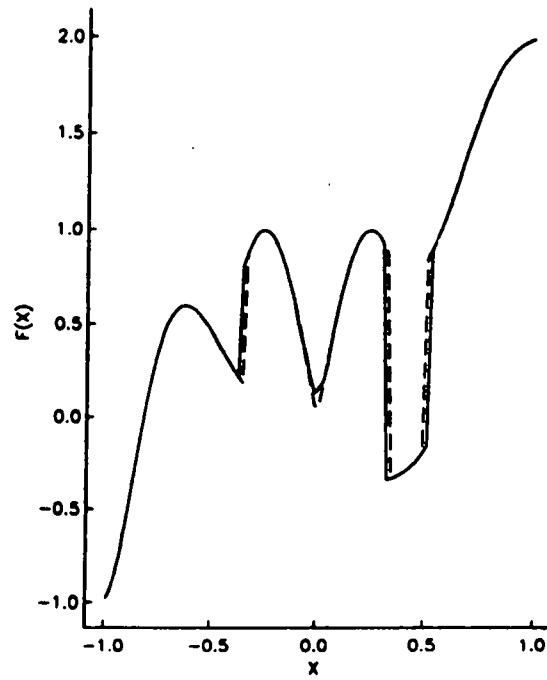


Figure 3.11: 3th order E.N.O. reconstruction with the 6400 nodes mesh from the deconvolution technique. Min=-1.325, Max=2.650,  $\delta = 0.8281 \cdot 10^{-2}$ .



(a) E.N.O. interpolation.



(b) E.N.O. reconstruction.

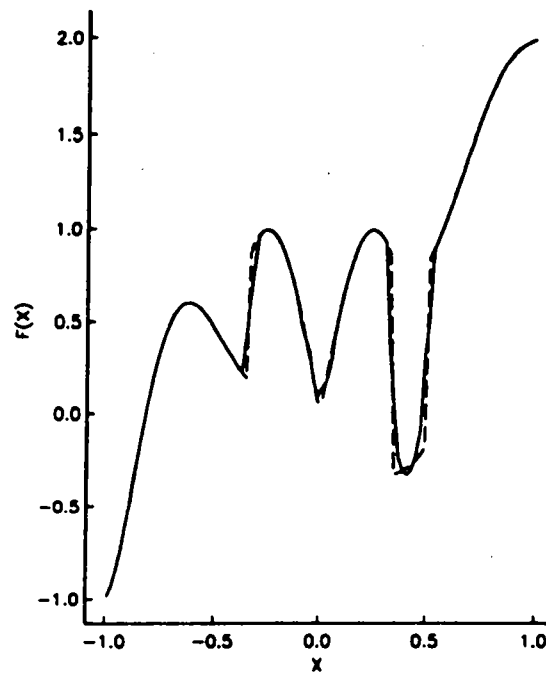
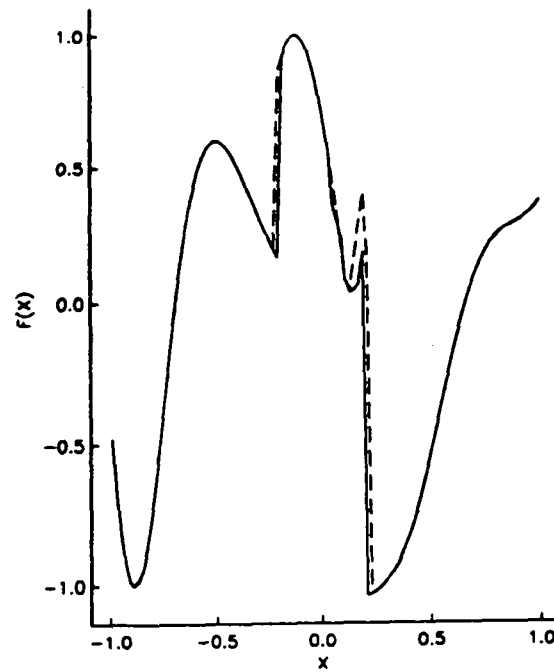


Figure 3.12: Cross-section at  $Y = 0$  of the E.N.O interpolation (a) and the E.N.O. reconstruction (b) for 1600 nodes the mesh.

(a) E.N.O. interpolation.



(b) E.N.O. reconstruction.

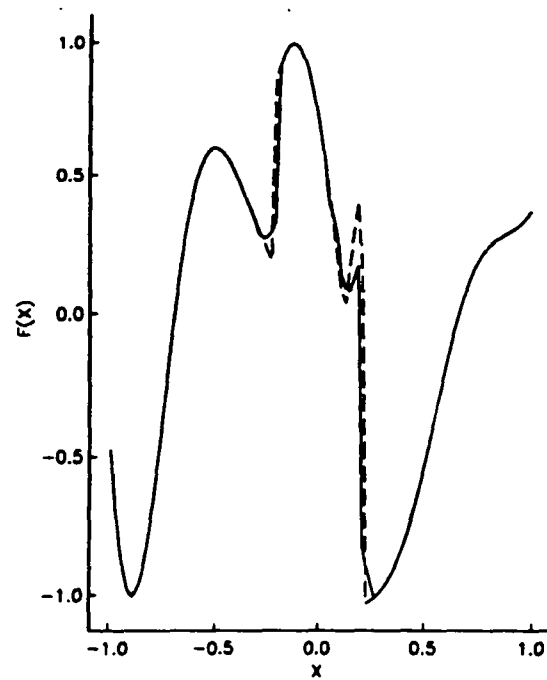


Figure 3.13: Cross-section at  $Y = 0.75$  of the E.N.O interpolation (a) and the E.N.O. reconstruction (b) for the 1600 nodes mesh. 47

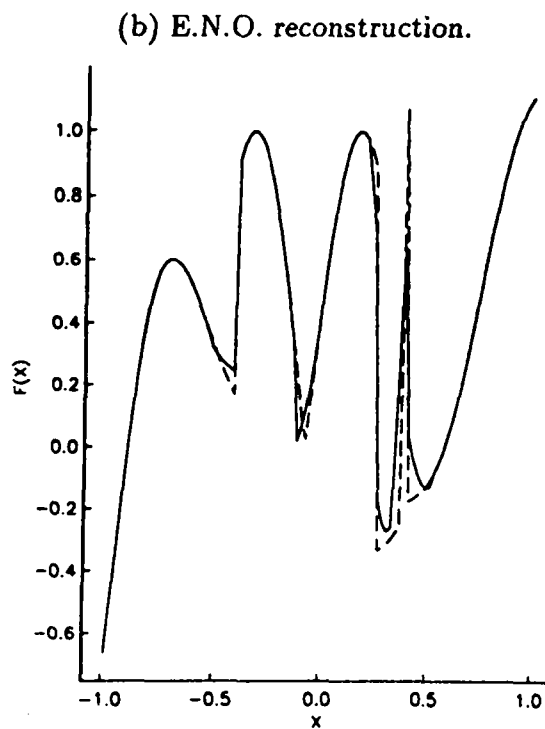
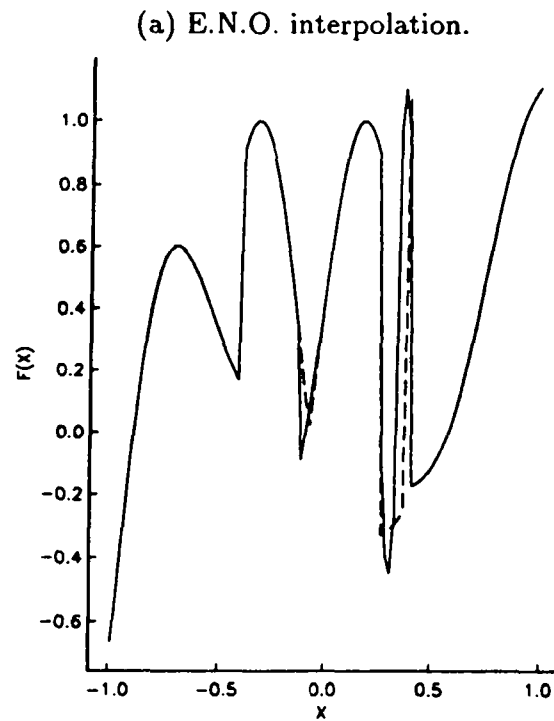


Figure 3.14: Cross-section at  $Y = -0.45$  of the E.N.O. interpolation (a) and the E.N.O. reconstruction (b) for the 1600 nodes mesh. 48

ISSN 0249-6399